Journal of Hydrology: Regional Studies 64 (2026) 103185

Contents lists available at ScienceDirect

Journal of Hydrology: Regional Studies

journal homepage: www.elsevier.com/locate/ejrh

Hydrological dynamics in a tropical peatland mosaic at Pulau Padang, Indonesia: Influence of land-cover changes and rainfall variability

Sofyan Kurnianto [a,*], Abdul Jabbar [a], Nurul A. Fitriyah [a], Adibtya Asyhari [a], Murugesan Balamurugan [b], Chandra P. Ghimire [c], Nurul Pertiwi [a], Ari P. Susanto [a], Atik Nurwanda [a], Steven Gunawan [a], Nurholis [a], Nardi [a], Yogi Suardiwerianto [a], Nurcahaya Simamora [a], Yuandanis W. Salam [a], Amit K. Haldar [a], Christopher D. Evans [d], Susan E. Page [e], Fahmuddin Agus [f], Dwi Astiani [g], Supiandi Sabiham [h], Symon Mezbahuddin [i,j], Chandra S. Deshmukh [a]

[a] *Asia Pacific Resources International Ltd., Pelalawan Regency, Indonesia*
[b] *DHI Water and Environment Pte. Ltd., Singapore, Singapore*
[c] *AgResearch, Lincoln Research Centre, Christchurch, New Zealand*
[d] *UK Centre for Ecology and Hydrology, Environment Center Wales, Bangor, United Kingdom*
[e] *School of Geography, Geology and the Environment, University of Leicester, Leicester, United Kingdom*
[f] *National Research and Innovation Agency, Cibinong, Indonesia*
[g] *Department of Forestry, University of Tanjungpura, Pontianak, Indonesia*
[h] *Department of Soil Science and Land Resources, IPB University, Bogor, Indonesia*
[i] *4S Analytics & Modelling Ltd., Edmonton, Canada*
[j] *Department of Renewable Resources, Faculty of Agricultural Life and Environmental Science, University of Alberta, Edmonton, Canada*

ARTICLE INFO

Keywords:
Hydrological modeling
Land-use
Climate
Subsidence
Inundation
Water management
Resilience

ABSTRACT

Study Region: Pulau Padang, Riau, Indonesia, a peat dominated island.
Study Focus: This study assessed hydrological dynamics under land-cover change and extreme rainfall variability using the coupled MIKE SHE–MIKE Hydro model. LiDAR, satellite imagery, and field measurements were used to quantify evapotranspiration, runoff, and storage change for 1972 (Past: counterfactual land-cover configuration), 2016 (Current), and 2066 (Future-policy compliance). All cases were driven by the 2015–2018 rainfall, covering the 2015 El Niño and the 2017 La Niña, to provide a representative window for evaluating interannual hydrological responses.
New hydrological insights for the region: Evapotranspiration represented 62–98 % of annual rainfall, the dominant water loss across all land-cover types. Conversion from peat swamp forest to managed areas caused ~1 % lower evapotranspiration, ~6 % higher runoff, and negligible differences in storage change under same rainfall inputs. In contrast, interannual rainfall variability produced up to eightfold differences in runoff and ~120 mm reversal in storage change between dry and wet years. Canal dams reduced groundwater drawdown to less than 5 cm within about 300 m of outermost canals, and forested peatlands buffered hydrological extremes. Inundation projections for 2066 show limited extent, with areas exceeding 1 cm depth for more than two

* Corresponding author.
E-mail address: sofyan_kurnianto@aprilasia.com (S. Kurnianto).

https://doi.org/10.1016/j.ejrh.2026.103185
Received 18 July 2025; Received in revised form 25 January 2026; Accepted 26 January 2026
Available online 17 February 2026

weeks remaining below 1 % of the managed landscape, suggesting limited long-term economic implications associated with inundation risk. The study highlights the importance of responsible peatland management.

1. Introduction

Peatlands play critical roles in providing economic, social and environmental services, including carbon and water cycle regulation (Harrison et al., 2019; Page et al., 2011). Southeast Asia hosts about one-third of the world's tropical peatlands (Gumbricht et al., 2017), with the majority formed between 17,000 and 4000 years ago following a sea-level high stand and under a relatively stable rainfall regime with a low intensity and frequency of drought (Dommain et al., 2011; Hapsari et al., 2022). Groundwater level (GWL) dynamics in these peatlands control geomorphology (Cobb et al., 2017), ecology (Nishimura et al., 2007), and biogeochemical cycles (Deshmukh et al., 2021; Page et al., 2022; Swails et al., 2018). In these rain-fed peatlands, seasonal and interannual GWL variations are influenced by rainfall (Cobb et al., 2017; Deshmukh et al., 2023; Hooijer, 2005). The rainfall variability is influenced by monsoonal pattern combined with El Niño–Southern Oscillation (ENSO), Indian Ocean Dipole (IOD) and Madden-Julian Oscillation (MJO) in Southeast Asia (Alsepan and Minobe, 2020; Amirudin et al., 2020; Hidayat and Kizu, 2010; Muhammad et al., 2020; Saji et al., 1999). In the recent decades, Southeast Asia has experienced increasingly frequent and severe El Niño events, often combined with the positive IOD phase, (Alsepan and Minobe, 2020; Xiao et al., 2022), leading to significant GWL drawdowns in tropical peatlands (Deshmukh et al., 2021; Hirano et al., 2012; Swails et al., 2018).

In addition, Southeast Asian peatlands have undergone significant land-cover changes driven by population growth and economic development (Miettinen et al., 2016). Approximately half of the region's peatlands are now managed for agriculture and silviculture (Miettinen et al., 2016; Wijedasa et al., 2018), forming a mosaic peatland landscape comprising peat swamp forests, smallholder farms, and industrial plantations. This mosaic configuration represents a spatially heterogeneous hydrological system in which natural and managed units coexist within the same catchment (Hardt et al., 2018; Vogt et al., 2024). Such heterogeneity alters vegetation cover and typically requires deeper groundwater levels compared to natural peat swamp forests. Changed plant area index, root systems (Zhang et al., 2001), and GWL can directly impact evapotranspiration rates (Deshmukh et al., 2023; Hirano et al., 2015). Water management practices using canal networks modify surface and subsurface runoff, as well as storage dynamics within and above the peat layer. Additionally, changes in land cover and management practices alter ground surface roughness (Dommain et al., 2010; Lampela et al., 2016), hydraulic conductivity due to increased peat bulk density (Anshari et al., 2010; Baird et al., 2017; Kurnianto, 2018; Rezanezhad et al., 2016), and surface elevation resulting from peat subsidence (Evans et al., 2019, 2022; Hooijer et al., 2012). These factors as well collectively influence surface runoff, subsurface runoff and storage processes (Baird et al., 2017; Wösten et al., 2006).

The groundwater level dynamics at the boundary between peat swamp forests and adjacent managed areas may be influenced by water management practices. Yet, the GWL dynamics in adjacent peat swamp forests and its governing factors are not well understood (Baird et al., 2017; Evans et al., 2022; Hooijer et al., 2012). Dams as one of the important water management structures, are commonly used to regulate water levels in managed peatlands, maintaining higher groundwater levels during dry seasons to reduce deeper GWL and facilitating drainage during wet seasons (Putra et al., 2021). While these infrastructures play a critical role in stabilizing hydrological conditions within managed areas, there remains limited understanding of their lateral impacts on groundwater dynamics in adjacent peat swamp forests (Putra et al., 2022). Specifically, the extent to which dams influence GWL fluctuations in neighboring ecosystems is poorly evaluated, highlighting the need for further investigation.

Prolonged inundation poses risks to crops and plantation growth. Given the low-lying nature of Southeast Asia's coastal peat landscapes, with ongoing peat subsidence (Evans et al., 2022), and sea level rise (Henman and Poulter, 2008), it is essential to resolve uncertainties in current and future inundation extent under intense and frequent extreme climate events in these economically important of managed landscape, but vulnerable (Lupascu et al., 2020).

Field measurements of rainfall, evapotranspiration, and GWL in forested peatlands present logistical challenges, further difficulty in capturing their spatial and temporal variability (Ismail et al., 2021). Measuring runoff is complicated by relatively flat topography and seasonal coastal riverbank flooding, which make it challenging to delineate catchment boundaries and determine cross-sectional flow areas (Hooijer, 2005). Consequently, empirical water balance assessments are limited in tropical peatlands in accounting for the combined effects of land-cover changes and climate anomalies (Deshmukh et al., 2021; Hirano et al., 2015; Tang et al., 2019). Hydrological modelling offers a valuable opportunity to address these challenges. Prior studies have applied physically-based models, e.g. SIMGRO (Wösten et al., 2006), Ecosys (Mezbahuddin et al., 2015, 2023) and SWAP (Taufik et al., 2019), to improve understanding of tropical peatland hydrology. However, application of fully physically based distributed hydrological models that explicitly integrate land-cover change, rainfall variability, groundwater-surface coupling and water management structures (such as canals and dams) in assessing key water balance components (evapotranspiration, runoff and storage change) using extensive field observations in tropical peatlands remain limited, particularly at the landscape scale and over multi-decadal timescales. Advancing a quantitative, process-based understanding of peatland hydrological responses to land-use change under current and near-future rainfall conditions is therefore crucial. This knowledge is essential for developing responsible peatland management strategies (Clarke and Rieley, 2019).

To address these gaps, we applied MIKE SHE coupled with MIKE Hydro software to simulate the hydrological processes of Pulau Padang, a peat-dominated island on the eastern coast of Sumatra, Indonesia (Fig. 1). To our knowledge, this represents one of the first landscape-scale applications of the MIKE SHE-MIKE Hydro modeling in a tropical peatland, explicitly resolving groundwater-surface

water interaction, canal and dam-based water management and long-term peat ground elevation change due to subsidence within a single, physically based and deterministic modeling system across the entire island. We integrated satellite imagery, airborne Light Detection and Ranging (LiDAR) data, and extensive field measurements of vegetation and peat properties across the island (Table 1). Utilizing these datasets, we pursued three main objectives: (1) to assess the impact of land-cover change and ground elevation lowering due to peat subsidence on water-balance components (evapotranspiration, runoff, and storage change) under the influence of

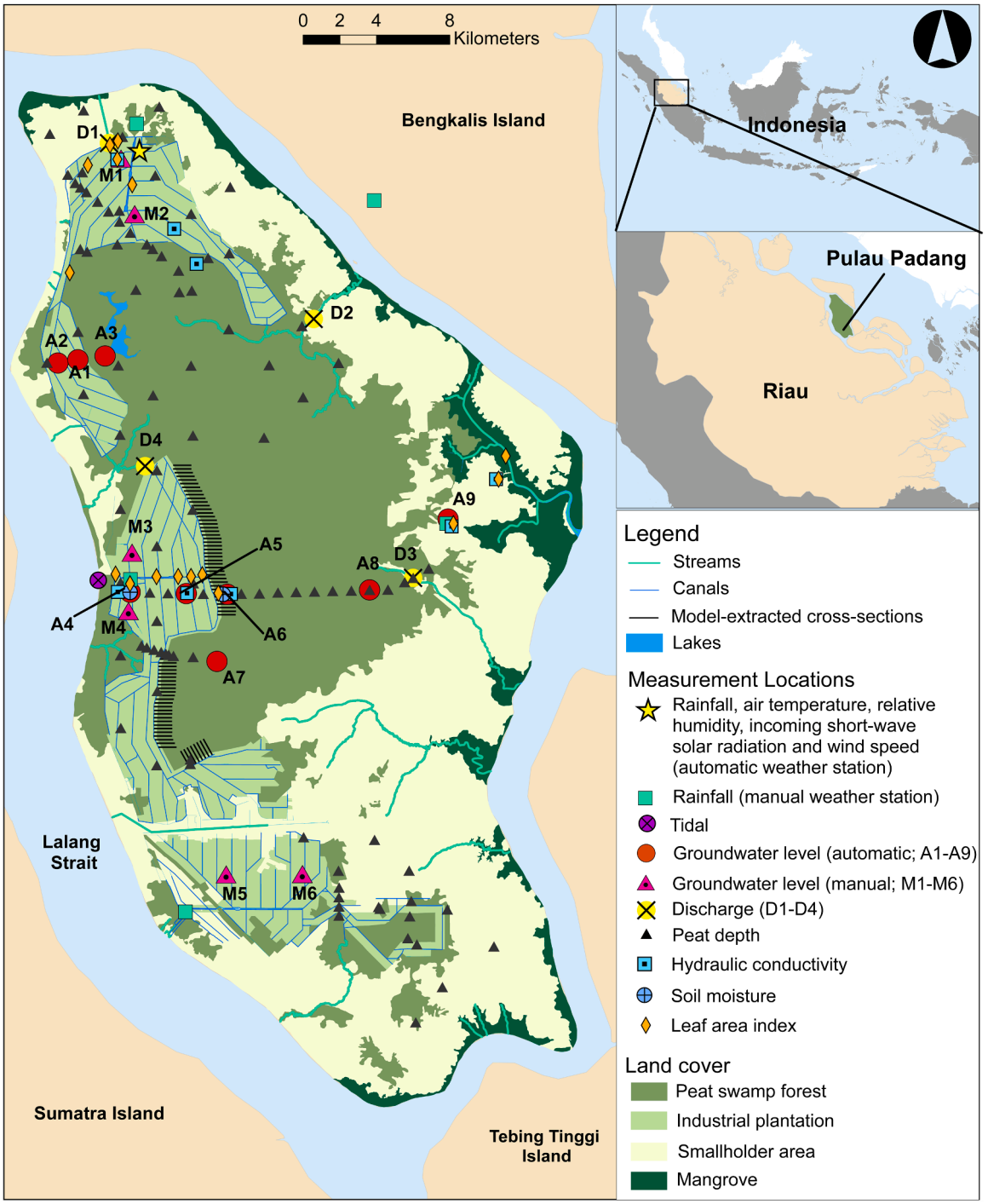

Fig. 1. Location of Pulau Padang, Riau, Indonesia, with 2016 land cover map. Field measurement locations for rainfall, air temperature, relative humidity, wind speed, net radiation, groundwater level, tide level, river and canal discharge, and vegetation and soil properties used in the modeling are indicated. Model-extracted cross-section depict the areas assessed for drainage impact in adjacent peat swamp forests in the model.

Table 1
Field measurement details, parameter ranges, and final calibrated values used for model setup. Range values represented minimum to maximum.

Model Input	Peat Swamp Forest	Smallholder Areas	Industrial Plantations	Mangroves	Methods
Land cover (km^2)					
1972	921	124	Not existed	63	Landsat 1 (EarthExplorer usgs.gov).
2016	409	449	188	63	Landsat 8 (EarthExplorer usgs.gov); Aerial photograph (Leica RCD30 60-megapixel metric medium format, Leica Geosystems AG, Switzerland).
2066	409	449	188	63	Assumed to be the same as 2016.
Ground elevation (m above sea level)					
1972	1.28 – 11.80	1.40 – 10.46	Not existed	1.18 – 7.77	Adjusted from 2016 elevation using constant subsidence rates from Hoyt et al. (2020) for smallholder areas and Evans et al. (2019) for industrial plantation. A primary subsidence of 0.75 m (Hooijer et al., 2012) was applied to industrial plantations, while a subsidence of 0.35 m was applied to smallholder areas.
2016	0.79 – 11.15	0.21 – 10.67	3.18 – 10.81	0.11 – 5.71	Airborne Light Detection And Ranging (Leica ALS-70 HP LiDAR system, Leica Geosystems AG, Switzerland) survey in 2016.
2066	0.49 – 9.85	0.21 – 9.10	1.87 – 9.21	0.11 – 5.06	Adjusted from 2016 elevation using subsidence rates from Evans et al. (2019), (2022).
Vegetation characteristics					
Plant area index (m^2 m^{-2})	5 (2.5 – 10)*	2.5 (1.3 – 5.0)*	3.5 (1.8 – 7.0)*	4 (2.0 – 8.0)*	LAI-2200C Plant Canopy Analyzer; calibrated in the model.
Root depth (m)	0.5 (0.25 – 1)*	0.6 (0.3 – 1.2)*	0.7 (0.4 – 1.4)*	1.0 (0.5 – 2.0)*	Destructive sampling was conducted for all land covers except peat swamp forests which use mean value of Brady (1997) and Sulistyanto (2004); calibrated in the model.
Overland flow properties					
Manning's roughness (s $m^{-1/3}$)	0.17	0.1	0.1	0.05	Surface roughness was determined with Manning's roughness utilizing method from Arcement and Schneider (1989).
Detention storage (m)	0.1 (0.05 – 0.1)*	0.05 (0.03 – 0.1)*	0.05 (0.03 – 0.1)*	0.1	Calibrated in the model.
Unsaturated zone soil properties					
Infiltration rate (m day^{-1})	86.4 (172.8 – 57.6)*	30.2 (60.4 – 20.1)*	17.2 (11.5 – 34.6)*	4.3 (2.9 – 8.6)*	Double ring infiltrometer and calibrated in the model.
Soil water content (m^3 m^{-3}):					
at saturated condition	0.88 (0.59 – 1.0)*	0.85 (0.57 – 1.0)*	0.86 (0.57 – 1.0)*	0.57 (0.38 – 1.0)*	Peat sampling with the gravimetric method; calibrated in the model.
at field capacity	0.73 (0.49 – 1.0)*	0.75 (0.50 – 1.0)*	0.71 (0.47 – 1.0)*	0.47 (0.31 – 0.94)*	
at wilting point	0.28 (0.19 – 0.56)*	0.28 (0.19 – 0.56)*	0.28 (0.19 – 0.56)*	0.2 (0.13 – 0.4)*	
Saturated zone soil properties					
Saturated horizontal hydraulic conductivity (m day^{-1}):					
Upper layer (0–1 m)	172.8 (86.4 – 345.6)*	51.84 (25.92 – 103.68)*	34.56 (17.28 –69.12)*	8.64 (4.32 – 17.28)*	Piezometer Slug test and calibrated in the model.
Middle layer (1–2 m)	69.12 (34.56–138.24)*	17.28 (8.64 – 34.56)*	17.28 (8.64 – 34.56)*	0.17 (0.09 – 0.3)*	
Lower layer (>2 m)	4.32 (2.16 – 8.64)*	4.32 (2.16 – 8.64)*	1.32 (0.66 – 2.64)*	0.17 (0.09 – 0.3)*	
Specific yield (-)	0.15 (0.08 – 0.3)*	0.1 (0.05 – 0.2)*	0.15 (0.08 – 0.3)*	0.1 (0.05 – 0.2)*	Calculated following Ismail et al. (2021) and calibrated in the model.
Specific storage (-)	0.015 (0.01 – 0.03)*	0.01 (0.01 – 0.02)*	0.015 (0.01 – 0.03)*	0.001 (0.001 – 0.002)*	Calibrated in the model.
Drainage level (m)	Not applied	–0.4 (–0.4 – –0.6)*	–0.4 (–0.4 – –0.6)*	Not applied	Calibrated in the model.
Time constant (s^{-1})	Not applied	2.00×10^{-5}	2.00×10^{-5}	Not applied	Calibrated in the model.
MIKE Hydro model parameters					
Bed resistance (s $m^{-1/3}$)	0.04				Resistance of stream bed was determined utilizing method from Arcement and Schneider (1989).
Leakage coefficient (-)	1.00×10^{-4} (5.00×10^{-5} – 2.00×10^{-4})*				Calibrated in the model.

* Range of calibration values are within the bracket

interannual rainfall variability, by comparing three modeling cases representing 1972 (Past), 2016 (Current), and 2066 (Future); (2) to evaluate the impact of canal dams on adjacent peat swamp forests by analyzing groundwater-level (GWL) dynamics near the outermost canals of managed areas; and (3) to quantify the spatial extent of inundation across the island under interannual rainfall variability. The year 2066 was selected as a 50-year projection from the 2016 baseline to represent long-term hydrological responses under modelled topographic changes caused by peat subsidence, while keeping land cover constant. All modelling cases were forced using the same meteorological dataset from 2015 to 2018, encompassing both dry and wet years, in order to isolate the structural hydrological effects of land-cover configuration, peat subsidence, and water-management infrastructure, rather than to represent historical or future climate trajectories. These objectives provide an integrated framework for understanding tropical peatland hydrology in Southeast Asia under combined influences of land-cover change and rainfall variability.

2. Methods

2.1. Study area

Pulau Padang is a 1100 km^2 island located off the eastern coast of Sumatra, Indonesia (Fig. 1). The island is predominately composed of peat resting on underlying marine clay, covering approximately 92 % of its surface. On the western coast, a sharp transition from peat to marine clay is largely driven by shoreline erosion along the narrow Lalang Strait (Brady, 1997). Conversely, the eastern coast exhibits a more gradual change in peat thickness. The mean peat depth is approximately 5 m, reaching 10 m at the deepest central locations. The island experiences a humid tropical climate, with mean monthly air temperatures ranging between 26 and 28°C. Rainfall seasonal and interannual patterns are influenced by monsoonal processes combined with El Niño–Southern Oscillation (ENSO) and Indian Ocean Dipole (IOD) (Alsepan and Minobe, 2020; Saji et al., 1999). Rainfall typically peaks in April and November, with monthly totals often exceeding 200 mm. Occurrence of strong El Niño events with a positive IOD phase lead to reduces annual rainfall (e.g. 2015 and 2019), while La Niña events with negative IOD increase rainfall (e.g. 2017 and 2022) (Sulaiman et al., 2023). From 2014–2023, mean annual rainfall was 2045 mm.

The island currently exhibits a mosaic land cover types with smallholder areas (40.4 % of the island area), peat swamp forest (36.7 %), industrial plantation (16.5 %), mangrove (5.7 %), and water bodies (0.7 %) (Fig. S1). The existing peat swamp forests are mostly situated in the central part of the island (Fig. S1), which can be classified as a mature peat swamp forest, encompassing both undisturbed peat swamp forest and peat swamp forest with historical logging activities, which has since regenerated to the point of being visually indistinguishable from undisturbed peat swamp forest (Wijedasa et al., 2018). Smallholder areas, which were first developed in the early 1970s through a nationwide transmigration program (Brady, 1997), include agricultural fields, rubber (Hevea brasiliensis) plantation, sago (Metroxylon sagu) farms and settlements (Fig. S1). The industrial plantation area was established in the early 2010s, primarily comprising fiber-wood Acacia crassicarpa and is concentrated in the island's western and northern regions (Fig. S1).

A network of natural streams and artificial canals currently spans Pulau Padang (Fig. S1). In the smallholder areas, canals are approximately 2 m wide and 1 m deep, with no regular water management infrastructures or practices and have a canal density of around 0.2 km km^{-2} (i.e., total canal length per square-kilometre of managed area). In contrast, industrial plantations have a more structured canal system (Fig. S1), organized within topographically defined water management zones. This system, used for transportation and GWL regulation purposes, includes three types of canals: main canal (~12 m wide), branch canal (~8 m wide), and perimeter canal (~6 m wide), all typically about 3 m deep, with a canal density of around 1.2 km km−2. Water flow and levels in these canals are regulated by adjustable dams to achieve GWL targets that support plantation growth. The industrial plantation was managed to maintain a GWL of around 0.4–0.8 m below the surface.

2.2. Field measurements for model setup

The model was set up using comprehensive field measurements as inputs (Table 1; Fig. S2). A detailed surface elevation map of the entire island was derived from a 1 m × 1 m grid size full-coverage airborne LiDAR survey (Leica ALS-70 HP LiDAR system, Leica Geosystems AG, Switzerland) conducted in 2016. Concurrently, digital aerial photographs (Leica RCD30 60-megapixel metric medium format, Leica Geosystems AG, Switzerland) were taken during the same survey, which were used to map the land cover, streams, and canals network (Fig. S1). Peat depth (m) measurements were taken at 102 sampling locations across all land covers within the island using a standard peat sampler (Peat Sampler Set, Royal Eijkelkamp, the Netherlands) in 2016.

Daily rainfall (mm) has been measured manually since January 2014 at five rain gauges located on and around the island (Fig. 1). All rainfall data from these gauges were quality-checked and verified against Indonesian Agency for Meteorological, Climatological, and Geophysics (BMKG) observations from Batam, ~320 km away from Pulau Padang (World Meteorological Organization station ID: 96087; Latitude 1.1167° N, Longitude 104.1167° E), showing consistent monthly and annual patterns for the 2014–2018 period. The year 2015 corresponded to a strong El Niño and positive Indian Ocean Dipole (IOD) event, representing an extyreme dry-year condition. An automatic weather station (Model ET107, Campbell Scientific, USA) was installed in January 2017 in the northern part of the island (Fig. 1), measured hourly air temperature (°C), relative humidity (%), wind speed (m s^{-1}), and net radiation (W m^{-2}).

In 2017 and 2018, peat physical, hydrological, and vegetation properties were measured across all land covers (Table 1 and Fig. 1).

Infiltration rates (m s^{-1}) were measured using a double ring infiltrometer. Water content (m^3 m^{-3}) at saturation and field capacity in the unsaturated peat layer were estimated using gravimetric method, with soil core samples taken from the peat layer above the GWL. Saturated horizontal hydraulic conductivity (m s^{-1}) was measured at the upper (0 – 1 m), middle (1 – 2 m), and lower (> 2 m) peat layers using a slug test, following Bouwer and Rice (1976) and adapted for tropical peatlands (Kurnianto et al., 2018). Manning's roughness (s $m^{-1/3}$) and surface detention storage (m) parameters were derived from Arcement and Schneider (1989) and model calibration. The plant area index (m^2 m^{-2}) was measured using an LAI-2200C Plant Canopy Analyzer (LI-COR, USA). Root depth (m) measurements were taken from the Kampar Peninsula using destructive sampling method (Sunaryathy et al., 2015) for the smallholder areas, industrial plantations, and mangroves, while the root depths for forests were taken from published literature (Brady, 1997; Sulistyanto, 2004).

Bi-weekly GWL measurements (m) were conducted manually from January 2017 to December 2018 at six locations within the industrial plantation (Fig. 1). To capture daily temporal variability, nine automatic water level loggers (Levelogger Edge 3001, Solinst, Canada) were installed to record hourly GWL: four in peat swamp forests, four in the industrial plantation, and one in smallholder areas (Fig. 1). Unfortunately, data for 2017 from one plantation site and one smallholder site were lost due to instrument failures. Monthly flow velocity (m s − 1) was measured using a flow meter (Braystoke Model 001, Valeport, UK), along with corresponding stream cross-sectional area (m^2) at four catchment outlets: two in natural streams and two within the industrial plantation, from January to December 2018 (Fig. 1). River and canal discharge were then calculated by multiplying flow velocity by cross-sectional area. Stream and canal geometries were measured in field during 2018, supplemented by aerial photographs from a 2016 survey for the inaccessible locations (Fig. 1). Bed resistance was assumed to be uniform across all channel types (Table 1), with values taken from Arcement and Schneider (1989).

Tide levels, representing the boundary condition, were measured on the island's western coast using an automatic water level logger (Levelogger Edge 3001, Solinst, Canada) (Fig. 1), which provides the most representative local signal of the semi-diurnal tide. Tidal measurements showed that the mean higher water level 1.15 m relative to mean sea level (Fig. S3), whereas the average ground elevation at approximately 100 m inland from the shoreline was 1.8 m along the island perimeter. We observed that the fluctuations were remain the same with daily amplitudes averaged at 1.12 m during the measurement period. This indicates that direct tidal inundation is confined to a narrow near-coastal fringe and that tidal influence inland is transmitted primarily through water levels in rivers and canals rather than through overland inundation across the peat surface. To assess potential spatial variation along the shoreline, we compared this record with a water level logger at Futong port, Kampar Peninsular, Sumatra, located approximately 43 km away. The Futong port record showed a tidal phase lag of about 1 h relative to the Pulau Padang logger. Given that the furthest point along the Pulau Padang coastline is within about 35 km of the island logger, the expected maximum tidal phase difference around the island is therefore less than 1 h. This is small relative to the daily timestep at which water balance components are analyzed in this study. Together, these findings support the assumption that the tidal signal measured at the island station provides an adequate first-order representation of tidal boundary conditions for the entire island.

2.3. Model setup

The MIKE SHE (DHI, 2017a) coupled with MIKE Hydro (DHI, 2017b), among the most sophisticated modeling softwares were used to simulate the hydrological processes of Pulau Padang. To resolve the complex interactions between surface and subsurface hydrological processes in peatland, together with their connectivity to managed canals and natural streams, this coupled modeling approach, which is fully physically based and deterministic, rather than data-driven or empirical modelling approach, is well suited for process-level analysis of water balance partitioning. The model represented the entire island as a single integrated hydrological domain rather than a homogeneous block, within which spatial heterogeneity in topography, vegetation, and soil properties was explicitly resolved. The model incorporated multiple drainage outlets, allowing rainfall to be routed according to natural flow directions and canal connectivity across the island. At each computational time step, the coupled MIKE SHE–MIKE Hydro system solved the surface and subsurface water flow equations for the entire island domain. Simulations were performed on a daily time step to capture the temporal variability in rainfall and its partitioning into evapotranspiration, runoff and storage change. Spatial variability in surface elevation, vegetation characteristics, and soil properties was incorporated using a horizontal grid resolution of 100 m × 100 m, totaling approximately 113,000 grid cells. These spatial and temporal resolutions were able to provide sufficient details for the scope of this study. Each grid cell was represented by a vertical column subdivided into three peat layers (0–100 cm, 100–200 cm, and >200 cm), capturing vertical variation in peat properties, while horizontal variation was defined by land-cover type (Table 1), with peat depth spatially interpolated using the Kriging method.

The rainfall input was derived using the area weighted mean rainfall from five rain gauges, calculated with the Thiessen polygon approach. Evapotranspiration was calculated as the sum of evaporation from the soil, open water and canopy, and transpiration from vegetation. The calculation of evapotranspiration was based on potential evapotranspiration (ET_p) and the water availability to meet ET_p requirements (Yan and Smith, 1994). ET_p was determined by multiplying reference evapotranspiration (ET_0) by a crop coefficient (K_c). ET_0 was computed using the FAO Penman-Monteith method (Allen et al., 1998) incorporating data on air temperature, relative humidity, wind speed, and net radiation from local weather stations within and around Pulau Padang. The K_c was derived from the relationship between the ET_0 and measured evapotranspiration using eddy covariance technique conducted nearby peatland area in the Kampar Peninsula, Sumatra, less than 100 km from Pulau Padang (Fig. S4; Deshmukh et al., 2023). ET_p is initially met by water from interception storage. If ET_p exceeds the available water from interception storage, it will then utilize ponded water. Should the requirement surpass the availability of both interception storage and ponded water, the unsaturated zone will supply the necessary water. If ET_p still exceeds the available water, it will be drawn from the saturated zone, contingent on the GWL (Yan and Smith, 1994).

To quantify runoff, MIKE SHE simulated both surface (overland) and subsurface (unsaturated in the uppermost peat layer, and saturated in the deeper peat layer) flows within model domain. The surface and subsurface flow outputs from MIKE SHE were coupled into stream and canal flows using one-dimensional channel flow routing within the MIKE Hydro model. To model the movement of ponded surface water, we used the finite difference approximation of the St. Venant equation to solve two-dimensional overland flow (Abbott et al., 1986b). Higher values for detention storage and surface roughness, which influence flow dynamics modeled by the St. Venant equations, were assigned to peat swamp forests compared to industrial plantation and smallholder areas (Table 1), reflecting differences in the microtopography. A one-dimensional vertical flow approach was employed to simulate water movement within the unsaturated zone, a method well-suited for areas with a shallow GWL, where actual evapotranspiration closely aligns with the reference evapotranspiration rate (Dai et al., 2010). This approach calculated both evapotranspiration and groundwater recharge (Yan and Smith, 1994) using plant area index, root depth, infiltration rate, and soil moisture content at wilting point, field capacity, and saturation (Table 1). The unsaturated zone was modelled in two layers: the upper layer, which handled infiltration and evapotranspiration, and the lower layer, which primarily governed percolation and groundwater recharge, with evapotranspiration in the lower layer considered negligible. In this study, groundwater recharge refers to vertical flow from the unsaturated to the saturated peat zone within the same column, since the peatland is ombrotrophic and underlain by an impermeable marine clay layer that prevents deeper percolation.

Storage change was calculated as the change in canopy, surface, and subsurface storage relative to their antecedent states. Saturated zone flow was modeled using the three-dimensional Darcy's equation, solved numerically through an iterative implicit finite difference approach (Abbott et al., 1986). Key inputs included horizontal hydraulic conductivity, vertical hydraulic conductivity, specific yield, and specific storage (Table 1). Vertical hydraulic conductivity was assumed to be half of the horizontal value (Lewis et al., 2011), as peat is an anisotropic medium (Beckwith et al., 2003). Specific yield and specific storage were calculated from rainfall and GWL, following the methodology of Ismail et al. (2021). Notably, storage change serves as a proxy for GWL fluctuations in the peat layer or above the ground surface. A negative storage change indicates GWL drawdown, while a positive storage change reflects a rise in GWL (Fig. S5).

Water levels in streams and canals were simulated as one-dimensional features in the MIKE Hydro model. This model required information on channel network and cross-section, bed resistance, and boundary conditions (Table 1). The surface and subsurface flows from MIKE SHE acted as lateral boundary conditions for the MIKE Hydro model. A constant no-flow boundary condition was applied to the upstream ends of the channels, while the measured tide levels were used at the downstream ends.

In Managed Area, canal dams are represented as structure elements within the MIKE HYDRO River network, reflecting the water-level control structures installed in the plantation canal system. A total of 123 dams were distributed along main, branch, and perimeter canals, aligned with operational water zoning. Each dam was parameterized as a full-width broad-crested weir with a fixed crest elevation set 0.6 m below the adjacent ground surface. When upstream water levels exceeded the crest elevation, flow passed over the structure according to the broad-crested weir equation. This configuration allowed the model to simulate water retention

Table 2
Model calibration and validation using measured groundwater level and discharge. Statistical performance metrics for model calibration (January-December 2017) and validation (January-December 2018) at each measurement location represented by significance of R^2, RMSE and NSE. Measurement locations (See Fig. 1) are identified as automatic (A1-A9) and manual (M1-M6) measurements for groundwater levels and D1-D4 for river and canal discharge measurements. N/A indicates unavailable measurements.

Measurement locations	Calibration (Jan - Dec 2017)		Validation (Jan - Dec 2018)		
	R^2	RMSE	R^2	RMSE*	NSE**
A1	0.77	0.07	0.69	0.09	0.56
A2	0.77	0.07	0.78	0.09	0.76
A3	0.73	0.04	0.44	0.09	0.36
A4	0.82	0.09	0.9	0.07	0.87
A5	0.72	0.05	0.77	0.05	0.72
A6	0.84	0.05	0.77	0.06	0.76
A7	0.75	0.04	0.89	0.06	0.84
A8	N/A		0.59	0.07	0.74
A9	N/A		0.81	0.07	0.6
M1	0.76	0.09	0.81	0.08	0.64
M2	0.8	0.06	0.85	0.08	0.62
M3	0.77	0.04	0.81	0.05	0.79
M4	0.89	0.07	0.96	0.08	0.68
M5	0.73	0.07	0.79	0.07	0.73
M6	0.71	0.05	0.91	0.05	0.66
D1	N/A		0.94	0.3	0.94
D2	N/A		0.98	0.32	0.95

Note: The baseline year (2016) defines the spatial distribution of land cover and ground elevation based on aerial photograph and LiDAR data and is independent of the calibration and validation periods. Groundwater level observations were not available in 2016 and therefore calibration was performed using data from subsequent years.

* RMSE value for groundwater level are in meter while river and canal discharge are in $m^3\ s^{-1}$.

** NSE is dimensionless.

upstream and controlled release downstream, thereby influencing groundwater levels across the managed landscape.

MIKE SHE and MIKE Hydro were dynamically coupled at each computational time step during the simulation. The coupling allows fully synchronous, two-way exchange of water fluxes between the one-dimensional (1-D) channel network in MIKE Hydro and the two-dimensional (2-D) overland and saturated zones in MIKE SHE River links, automatically generated from MIKE Hydro channel coordinates, define the hydraulic interface between channel reaches and adjacent MIKE SHE grid cells. During each time step, MIKE Hydro transfers simulated water levels from its channel nodes to the corresponding river links in MIKE SHE, while MIKE SHE returns overland- and groundwater-exchange fluxes to MIKE Hydro for the next step. Channel overflow and reverse flow occur whenever simulated water levels exceed local bank elevations, allowing realistic bidirectional flow between channels and floodplains (DHI, 2017c).

2.4. Model performance evaluation

We used a split-sample approach for model calibration and validation (Refsgaard, 1997). The year 2014 was treated as a warm-up period to establish initial conditions for the model. Calibration was conducted using GWL measurements from January to December 2017, corresponding to the first year with GWL measurement available for model evaluation. Validation was performed for January to December 2018, the year with concurrent observations of both GWL and river and canal discharge, by comparing modeled and measured both variables (Fig. 1; Table 2). Parameter optimization during calibration was based on the root mean squared error (RMSE) and coefficient of determination (R^2) (Table 2). Given the coupled nature of the model, simultaneous calibration of both the MIKE SHE and MIKE Hydro models was necessary, as changes to a calibration parameter in one model could influence results in the other (Thompson et al., 2004). Model performance during validation was assessed using R^2, RMSE, and the Nash-Sutcliffe Efficiency coefficient (NSE), a widely applied coefficient for evaluating hydrological model performance. An NSE value exceeding 0.5 indicates satisfactory model performance (Knoben et al., 2019; Moriasi et al., 2007). The water-balance calculation was iterated 200 times to ensure mass-balance convergence between rainfall input and simulated outputs (evapotranspiration, runoff, and storage change). The resulting residual errors were below 0.2 % of total rainfall, confirming numerical stability rather than over-calibration or overfitting, and within the acceptable 1 % threshold (Rahim et al., 2012).

2.5. Water balance components under Current, Past and Future

Evapotranspiration, runoff, and storage change were extracted directly from MIKE SHE model outputs for 1972 (Past), 2016 (Current), and 2066 (Future). The baseline year 2016 (Current) defines the spatial distribution of land cover and ground elevation based on the most recent aerial photograph and LiDAR data, respectively. The Past case refers to a counterfactual sensitivity analysis in which the 1972 land-cover configuration and reconstructed ground elevation were simulated under the same 2015–2018 meteorological forcing used for the Current and Future cases, rather than a historical reconstruction of 1972 climate conditions. The Future case was defined as a policy-compliance scenario, in which land cover is assumed to remain unchanged from the 2016 baseline. The year 2066 of Future represents a 50-year projection from 2016, selected to represent a multi-decadal horizon to assess long-term hydrological responses to cumulative peat ground elevation lowering due to subsidence (e.g. Hein et al., 2022), rather than to provide a deterministic future climate or land-use change projection. The simulations incorporated land-cover maps from 1972 and 2016, while the 2066 case maintained the 2016 land-cover.

For Past, Current, and Future, we used the same meteorological data (rainfall, air temperature, relative humidity, wind speed, and net radiation) from 2015 to 2018, which encompassed climate anomalies: El Niño combined with a positive Indian Ocean Dipole in 2015 (a hydrological dry year) and La Niña in 2017 (a hydrological wet year), targeting the same rainfall variability to interact with land-cover changes, on-going peat ground lowering and sea-level rise as boundary conditions. This consistent meteorological forcing allows isolation of hydrological responses to land-cover change and peat ground elevation lowering under identical interannual rainfall variability, framing the simulations as a process-based hydrological sensitivity analysis rather than a representation of historical or future climate trajectories (see Li et al., 2007). Notably, the Future rainfall projections for the study area for 2060 s, based on the Coupled Model Intercomparison Projects 6 (CMIP6) under Representative Concentration Pathway (RCP 8.5) with ensembles from 27 models, indicated potential interannual rainfall variability similar to the 2015 and 2017 conditions (Fig. S6).

For the Current, land cover and ground elevation were derived from the 2016 LiDAR survey. The Past case utilized 1972 land cover from Landsat 1 satellite imagery (Fig. S1), with elevation adjustments based on peat subsidence rates applied to the 2016 LiDAR data to represent Past ground elevation. We applied constant subsidence rates of 0.043 m $year^{-1}$ for industrial plantation areas (Evans et al., 2019) and 0.017 m $year^{-1}$ for smallholder areas (Hoyt et al., 2020). In addition, we included primary subsidence values of 0.75 m (Hooijer et al., 2012) and 0.35 m to represent rapid primary consolidation occurring during the early years following conversion of peat swamp forests to industrial plantation and smallholder areas, respectively. No subsidence was assumed for peat swamp forests from the Current to the Past case.

For the Future case, we assumed the Current (2016) land cover remains unchanged, consistent with the Indonesian government's peatland deforestation moratorium (Presidential Decree No. 8 of 2015) and the designation of most of the remaining peat swamp forest on the island as an 'Ecosystem Restoration' concession. This Future case therefore represents a policy-compliance trajectory, assuming stable land cover, minimal changes in peatland utilization and its associated water management structure under existing governance frameworks. The 2016 LiDAR elevation was adjusted to reflect the 2066 case by incorporating exponentially declining peat subsidence rates (Evans et al., 2019, 2022). The subsidence rates applied from Current to Future reflect ongoing peat compaction and oxidation processes occurring within the existing land-cover types under existing management, rather than subsidence associated with new

land-use conversion. Compaction reflects volume reduction of peat caused by surface loading, for example from infrastructure and operational activities, and shrinkage during drying, while oxidation reflects organic matter decomposition in the aerated zone above the water table and associated carbon loss as CO_2 emissions (Hooijer et al., 2012). We also applied a projected sea level rise of 6.4 mm year^{-1} under RCP 8.5 (Church et al., 2013; Mbow et al., 2017) to represent the potential Future hydraulic gradients. Cross-section data for the streams and canals were adjusted based on the adjusted elevation to ensure representative hydrological dynamics and flow capacities under Past and Future cases.

ForPast, Current, and Future, the water balance is expressed conceptually as rainfall being portioned into evapotranspiration, runoff and changes in total water storage, aggregated across three land-cover categories representing different management practices: i) Forest: natural peat swamp forest areas; ii) Managed Area: smallholder areas and industrial plantations; iii) Entire Island, offering a comprehensive landscape-level perspective. In the MIKE SHE, infiltration, percolation and groundwater recharge are resolved internally as vertical fluxes between the unsaturated and saturated peat layers and are therefore not reported as separate water-balance components. Instead, their net effect is reflected in the storage change term, which integrates changes is canopy, surface, and groundwater storage, and closely corresponds to simulated GWL dynamics. Within the Forest category, we further classified sub-categories to capture key differences: Forest (Peat Dome), representing extensive, contiguous, and mature peat swamp forests located in the center of the island, and Forest (Converted to Managed Area between 1972 and 2016), referring to natural forests converted to managed areas during this period. Similarly, within the Managed Area category, we added the subcategory Managed Area (Established Between 1972 and 2016), representing smallholder areas and industrial plantations developed during this timeframe. Additionally, we conducted simulations to compare Current water balance components in the absence of dam. This allowed us to assess the influence of such infrastructures on hydrological processes.

Statistical significance of differences in water balance components due to interannual rainfall variability and landcover change was evaluated using one-way ANOVA and independent-samples *t*-tests, respectively. The normality of data distribution was verified prior to analysis using the Shapiro–Wilk test. All descriptive statistics are reported as mean ± standard deviation (SD), representing interannual variability among modeled years unless otherwise specified.

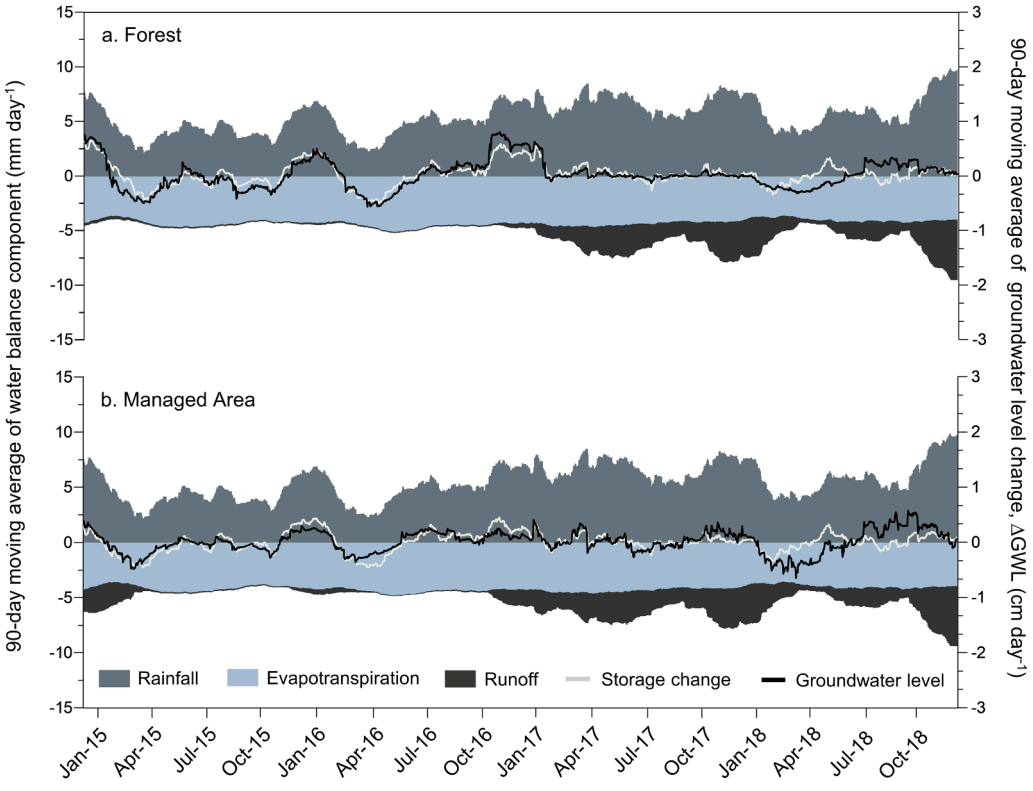

Fig. 2. Ninety day moving average of rainfall, evapotranspiration, runoff, groundwater level change, and total storage change from January 2015 to December 2018 in Pulau Padang, Riau, Indonesia. Panels represent the two model domains, (a) Forest and (b) Managed Area. Rainfall, evapotranspiration, runoff, and storage change are presented in mm day^{-1} using the left vertical axis, while groundwater level change is presented in cm day^{-1} using the right vertical axis. Positive and negative for values of water balance components represent inputs to and outputs from the ecosystem, respectively. Rainfall, evapotranspiration, runoff, and storage change are displayed as stacked bar components.

2.6. Inundation extent and impact of drainage in Managed Area on GWL in adjacent forest

In our study, inundation was defined as GWL exceeding 1 cm above the surface, based on prior studies (Sandi et al., 2019). Using criteria from Hein et al. (2022), which indicated that inundation lasting over two weeks lead to reduced productivity in Sumatra's agricultural areas, we calculated inundation extent by counting grid cells where the GWL remained this threshold for more than two weeks annually.

The drainage impact analysis evaluated GWL change and its extent from the outermost canal in managed areas toward the adjacent peat swamp forest. Using a high-resolution 25 m × 25 m grid, we extracted 75 cross-sections, spaced 200 m apart and extending 1 km from the outermost canal from the model (Fig. 1). The drainage impact in the adjacent peat swamp forest was determined by comparing the simulated GWL with and without canals in the Managed Areas. Further, we assessed the influence of water management infrastructure by simulating GWL with and without canal dams.

3. Results

3.1. Model performance in simulating GWL and discharge

Our results demonstrated the model's ability to simulate a wide range of GWL dynamics, spanning from deeper GWL in the dry periods to shallower GWL in wet periods in the forests, industrial plantations, and smallholder areas (Fig. 1; Table 2). During the model calibration, we found strong correlations between the measured and simulated GWL with low RMSE values at all GWL measurement locations (Table 2). The validation period also showed strong correlations and low RMSE for all GWL measurements, and river and canal discharge measurements. Additionally, the NSE exceeded 0.5 for all GWL and discharge measurement locations (Table 2).

3.2. Water balance components under Current case

Daily evapotranspiration often exceeded daily rainfall, occurred on approximately 58 % of days during a wet year and up to 72 % during a dry year across the Forests, Managed Area and the Entire Island (Fig. 2). Notably almost all rainfall was returned as evapotranspiration in the dry year of 2015 regardless of the land cover. In the Forest (Peat Dome), annual evapotranspiration ranged from 1451 (65 % of total annual rainfall) to 1643 mm (93 % of total annual rainfall), which shows statistical significance ($p < 0.05$). Similarly, evapotranspiration in Managed Area ranged from 1447 (64 % of total annual rainfall) to 1600 mm (90 % of total annual rainfall) (Table 3), also showing statistical significance ($p < 0.05$). Consequently, annual evapotranspiration across the Entire Island ranged from 1449 (64 % of total annual rainfall) to 1612 (91 % of total annual rainfall) (Table 3), which shows statistical significance ($p < 0.05$). This indicates that evapotranspiration accounted for the largest proportion of rainfall partitioning among water-balance components, remaining consistently high regardless of seasonal and interannual rainfall variability (Fig. 2; Fig. S7).

Runoff dynamics within the Forest (Peat Dome), Managed Area, and Entire Island exhibited significant seasonal and interannual variability closely following the rainfall pattern ($p < 0.05$) (Fig. 2; Fig. S7). Runoff was typically lowest during the dry period and peaked during the wet period across all land covers (Fig. 2). In the Forest (Peat Dome), runoff remained low (< 1 mm day^{-1}) throughout the dry year, while during the wet year, it reached up to 24 mm day^{-1}. Annual runoff in the Forest (Peat Dome) during the wet year was 856 mm (34 % of the total annual rainfall), 16 times greater than in the dry year (54 mm, 4 % of total rainfall) (Table 3). In the Managed Area, daily runoff was remained below 14 mm day^{-1} in the dry year, but reached up to 32 mm day^{-1} during the wet year. Annual runoff in the Managed Area during the wet year was 880 mm (35 % of total rainfall), about 10 times higher than in the dry year (89 mm, 6 % of total rainfall) (Table 3). Although the Managed Area produced slightly higher runoff than the forest under similar rainfall conditions due to lower surface roughness and more efficient drainage connectivity, the difference annual runoff between land-cover types, i.e. 450 ± 448 mm $year^{-1}$ and 489 ± 417 mm^{-1} in Forest and Managed Area, respectively (approximately 8 %) was minor compared with the much larger interannual variation (~800 mm) caused by rainfall differences between dry and wet years in both land cover types. Overall, the annual runoff across the Entire Island ranged from 98 mm (6 % of total rainfall) in the dry year to 868 mm (35 % of total rainfall) in the wet year (Table 3; Fig S7) and was consistently the second largest components of rainfall partitioning on annual basis, irrespective of land cover.

Similar to runoff, storage change showed significant seasonal and interannual variability regardless of land cover (Fig. 2; Fig. S7). In the Forest (Peat Dome) during the dry year, annual storage change was −55 mm (for which negative storage change values indicate storage depletion and positive values indicate storage accumulation), with GWL ranging from −59 to 10 cm (Fig. 2; Table 3). In contrast, during the wet year, annual storage change in the Forest (Peat Dome) was 82 mm, with GWL ranging from −2 to 14 cm (Fig. 2; Table 3). Similarly, in the Managed Area, annual storage change was −56 mm during the dry year, with GWL ranging from −98 to −46 cm (Fig. 2; Table 3). During the wet year, annual storage change in the Managed Area was 67 mm, with GWL remained below the ground, ranging from −74 to −38 cm (Fig. 2; Table 3). Overall, across the Entire Island, storage change was −70 mm $year^{-1}$ during the dry year and 74 mm $year^{-1}$ during the wet year (Table 3).

In the absence of dams in the water management infrastructure of the Managed Area, annual evapotranspiration decreased from 1499 to 1484 mm during the dry year, while runoff and storage depletion increased from 89 to 114 mm and from −49 to −60 mm, respectively, compared to the Current case with dams (Table S1). Overall, comparison between with and without dam, the annual evapotranspiration decreased from 1523 ± 65 to1515 ± 62 mm, runoff increased from 489 ± 417496 ± 403 mm, however storage change did not alter significantly from 0 ± 47–1 ± 56 mm (Table S1).

Table 3
Annual water balance components in 1972 (Past), 2016 (Current), and 2066 (Future), simulated under identical 2015–2018 meteorological data. The Past and Future represent counterfactual and policy-compliance sensitivity scenarios, respectively. 2015–2018 served as Year 1 – 4, with Year 1 representing a hydrologically dry period and Year 3 a hydrologically wet period. Percentages represent each component's proportion of total rainfall. Values are shown as mean ± standard deviation (SD).

	Land Cover	Water Balance Components (mm)	Year 1	Year 2	Year 3	Year 4	Average ± SD
	All	Rainfall	1538	1772	2490	2248	2012 ± 435
1972 (Past)	Entire Island	Evapotranspiration	1522 (99 %)	1622 (92 %)	1553 (62 %)	1451 (65 %)	1537 ± 71
		Runoff	72 (5 %)	108 (6 %)	853 (34 %)	815 (36 %)	462 ± 430
		Storage Change	−57 (-4 %)	43 (2 %)	86 (3 %)	−18 (−1 %)	13 ± 64
	Forest (Total)	Evapotranspiration	1523 (99 %)	1623 (92 %)	1553 (62 %)	1451 (65 %)	1530 ± 69
		Runoff	81 (5 %)	99 (6 %)	838 (34 %)	813 (36 %)	478 ± 414
		Storage Change	−67 (−4 %)	51 (3 %)	100 (4 %)	−16 (−1 %)	5 ± 60
	Forest (Peat Dome)	Evapotranspiration	1538 (100 %)	1642 (93 %)	1552 (62 %)	1452 (65 %)	1546 ± 78
		Runoff	44 (3 %)	69 (4 %)	858 (34 %)	818 (36 %)	447 ± 452
		Storage Change	−45 (-3 %)	62 (4 %)	80 (3 %)	−22 (−1 %)	19 ± 62
	Forest (converted to managed between 1972 and 2016)	Evapotranspiration	1514 (98 %)	1609 (91 %)	1554 (62 %)	1451 (65 %)	1532 ± 67
		Runoff	107 (7 %)	115 (7 %)	825 (33 %)	809 (36 %)	464 ± 408
		Storage Change	−84 (−5 %)	48 (3 %)	114 (5 %)	−12 (-1 %)	17 ± 84
	Managed Area (Total)	Evapotranspiration	1505 (98 %)	1603 (90 %)	1550 (62 %)	1452 (65 %)	1528 ± 65
		Runoff	74 (5 %)	173 (10 %)	882 (35 %)	811 (36 %)	485 ± 421
		Storage Change	−41 (−3 %)	-3 (0 %)	57 (2 %)	−15 (−1 %)	0 ± 41
2016 (Current)	Entire Island	Evapotranspiration	1510 (98 %)	1612 (91 %)	1549 (62 %)	1449 (64 %)	1530 ± 69
		Runoff	98 (6 %)	142 (8 %)	868 (35 %)	803 (36 %)	478 ± 414
		Storage Change	−70 (−5 %)	18 (1 %)	74 (3 %)	−4 (−0 %)	5 ± 60
	Forest (Peat Dome)	Evapotranspiration	1538 (100 %)	1643 (93 %)	1552 (62 %)	1451 (65 %)	1546 ± 79
		Runoff	54 (4 %)	71 (4 %)	856 (34 %)	820 (36 %)	450 ± 448
		Storage Change	−55 (−4 %)	59 (3 %)	82 (3 %)	−24 (−1 %)	16 ± 66
	Managed Area (Total)	Evapotranspiration	1499 (97 %)	1600 (90 %)	1547 (62 %)	1447 (64 %)	1523 ± 65
		Runoff	89 (6 %)	172 (10 %)	880 (35 %)	817 (36 %)	489 ± 417
		Storage Change	−49 (−3 %)	0 (0 %)	63 (3 %)	−15 (−1 %)	0 ± 47
	Managed area (established between 1972 and 2016)	Evapotranspiration	1495 (97 %)	1596 (90 %)	1546 (62 %)	1446 (64 %)	1521 ± 65
		Runoff	99 (6 %)	173 (10 %)	877 (35 %)	819 (36 %)	492 ± 413
		Storage Change	−56 (−4 %)	4 (0 %)	67 (3 %)	−16 (−1 %)	0 ± 51
2066 (Future)	Entire Island	Evapotranspiration	1504 (98 %)	1605 (91 %)	1549 (62 %)	1448 (64 %)	1526 ± 67
		Runoff	95 (6 %)	148 (8 %)	866 (35 %)	817 (36 %)	482 ± 417
		Storage Change	−61 (−4 %)	19 (1 %)	76 (3 %)	−17 (−1 %)	4 ± 58
	Forest (Peat Dome)	Evapotranspiration	1539 (100 %)	1641 (93 %)	1552 (62 %)	1452 (65 %)	1546 ± 78
		Runoff	58 (4 %)	77 (4 %)	856 (34 %)	820 (36 %)	453 ± 445
		Storage Change	−60 (−4 %)	54 (3 %)	83 (3 %)	−24 (−1 %)	13 ± 66
	Managed Area (Total)	Evapotranspiration	1492 (97 %)	1594 (90 %)	1547 (62 %)	1446 (64 %)	1520 ± 64
		Runoff	97 (6 %)	178 (10 %)	878 (35 %)	817 (36 %)	493 ± 412
		Storage Change	−51 (−3 %)	0 (0 %)	65 (3 %)	−15 (−1 %)	0 ± 48

Note: The water balance is interpreted conceptually as rainfall input being partitioned into evapotranspiration, runoff, and storage change, which integrates changes in canopy, surface, and subsurface storage. Infiltration, percolation, and groundwater recharge are resolved internally within MIKE SHE and are therefore reflected in storage change rather than reported as separate water-balance components.

3.3. Land-cover change impacts on water balance components

The comparison of the Entire Island under the Past and Current land-cover distribution, simulated under the same meteorological forcing, shows that annual evapotranspiration slightly decreased from 1537 ± 71 to 1530 ± 69 mm, but this difference was not statistically significant ($p > 0.05$). A similar pattern was observed seasonally, with a more pronounced reduction during the dry year (from 1522 to 1510 mm) compared to the wet year (from 1553 to 1549 mm). Annual runoff increased slightly from 462 ± 430 to 478 ± 414 mm, but the difference was not significant ($p > 0.05$) and was observed in both the dry year (from 72 to 98 mm) and the wet year (from 853 to 868 mm). Storage change lowered marginally from 13 ± 64 to 5 ± 60 mm, with higher depletion in the dry year (from −57 to −70 mm) and lower accumulation in the wet year, but none of these differences were statistically significant (from 86 to 74 mm) (Fig. 3; Table 3).

The Forest (Peat Dome) showed negligible changes in evapotranspiration, runoff, and storage dynamics, with no significant interannual variability (Fig. 3; Table 3). When comparing the Forest (converted to managed area between 1972 and 2016) under the Past land-cover distribution to the Managed Area (established between 1972 and 2016) under the Current case, annual evapotranspiration decreased slightly, but was not statistically significant ($p > 0.05$) from 1532 ± 67 to 1521 ± 65 mm (Fig. 3), with a more pronounced reduction during the dry year (from 1514 to 1495 mm) compared to the wet year (from 1554 to 1546 mm) (Table 3). Annual runoff increased slightly from 464 ± 408 to 492 ± 413 mm (Fig. 3), with a decrease in the dry year (from 107 to 99 mm), but an increase in the wet year (from 825 to 877 mm), although these changes were not statistically significant ($p > 0.05$). Storage change lowered from 17 ± 84 to 0 ± 51 mm, with a notable lower accumulation in the wet year (from 114 to 67 mm), and lower depletion in the dry year (from −84 to −56 mm) (Table 3), but again without significant difference ($p > 0.05$).

The comparison between the Current and Future cases revealed minimal changes and statistically insignificant differences in annual evapotranspiration, runoff and storage change across the Forest (Peat Dome), Managed Area, and Entire Island ($p > 0.05$; Fig. 3 and Table 3). In the Forest (Peat Dome), evapotranspiration remained nearly unchanged, from 1546 ± 79 to 1546 ± 78 mm, annual runoff showed a slight increase from 450 ± 448 to 453 ± 445 mm, and storage change varied slightly from 16 ± 66 to 13 ± 66 mm between the Current case to the Future case (Fig. 3). In the Managed Area, evapotranspiration decreased marginally from 1523 ± 65 mm in the Current to 1520 ± 64 mm in the Future case, while runoff increased slightly from 489 ± 417 to 493 ± 412 mm, and storage change remained stable from 0 ± 47 to 0 ± 48 mm (Fig. 3). These small changes in water balance components at the Forest (Peat Dome) and Managed Area (Total) level led to negligible differences in evapotranspiration (1530 ± 69 to 1526 ± 67 mm), runoff (478 ± 414 to 482 ± 417 mm) and storage change (5 ± 60 to 4 ± 58 mm) across the Entire Island (Fig. 3), all of which were statistically insignificant ($p > 0.05$).

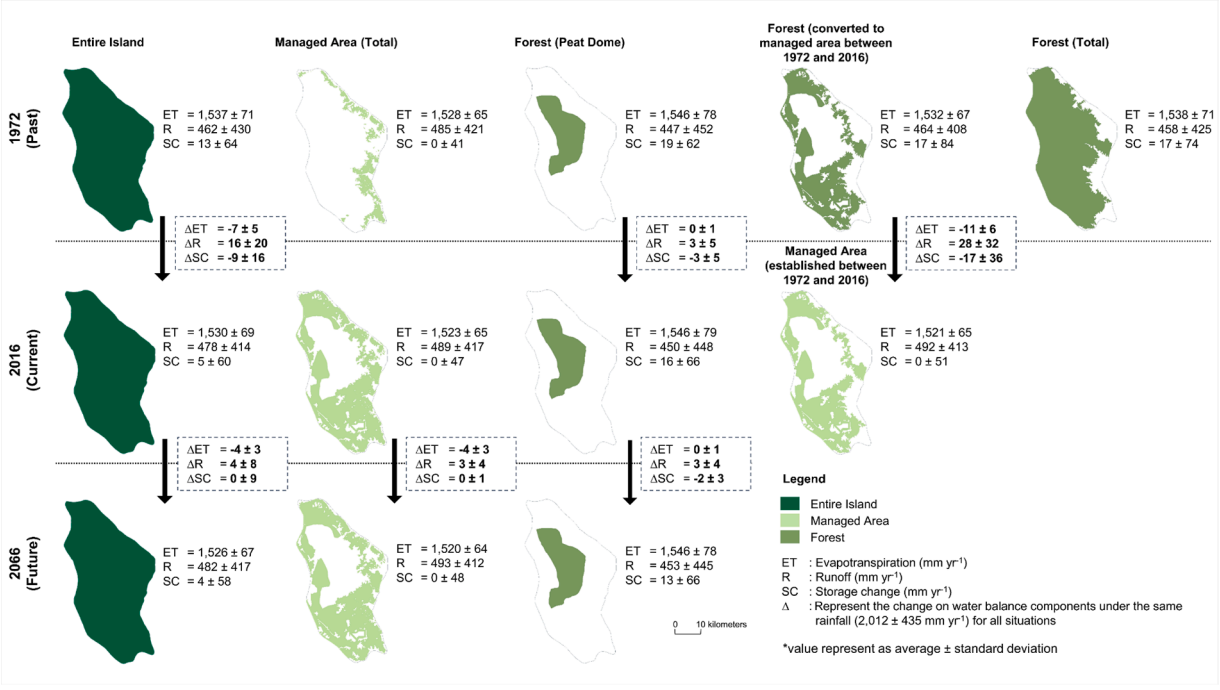

Fig. 3. Water balance components for 1972 (Past), 2016 (Current), and 2066 (Future) in Pulau Padang, Riau, Indonesia, simulated under identical 2015–2018 meteorological forcing. The Past case represents a counterfactual sensitivity experiment based on the 1972 land-cover spatial distribution, while the Future case represents a policy-compliance scenario based on the 2016 land-cover configuration with adjusted peat ground elevation. Bold values indicate changes in water balance components between cases.

3.4. Drainage impact on GWL in adjacent peat swamp forest

The results show that the drainage impact (ΔGWL) decreased following a power-law relationship with distance from the outermost canal, averaging 9 cm at 100 m and falling below 5 cm at approximately 300 m where dams were present. In the absence of dams, the drainage impact was stronger, averaging 19 cm at 100 m and extending beyond 300 m into the adjacent forest. The results also suggest a leveling off of drainage impacts beyond 300 m but these effects never approached zero, even at 1 km into the adjacent forest (Fig. 4). This finding is consistent with prior studies (Evans et al., 2019, 2022). The level off at < 5 cm drawdown value also fell within observed RMSE of GWL measurements in the peat swamp forest during calibration and the validation period (Table 2). In the absence of dams, the magnitude and extent of the drainage impact reached much farther into the adjacent peat swamp forest (Fig. 4), highlighting the significant influence of dams in water management within the Managed Area and their influence on the hydrology of the adjacent peat swamp forest.

3.5. Inundation extent

Inundation areas were predominately observed in the Forest for both the Current and Future cases (Fig. 5; Fig. 6). Inundation area in Managed Area remained limited (<1 %) regardless of rainfall variabilities. In the wet year, the inundation area in industrial plantation was 0.15 % (94 ha) of the total managed area in the Current case and changed to 0.19 % (123 ha) in the Future case (Fig. 6). During the dry year, the inundation area was covering only 0.01 % (8 ha) in the Current case and shifted to 0.10 % (64 ha) the Future case. For smallholder areas, the wet year inundation area was 0.26 % (164 ha) of the total managed area in the Current case, with a change to 0.33 % (211 ha) in the Future case. During the dry year, inundation in smallholder areas changed from 0.07 % (46 ha) in the Current case to 0.30 % (192 ha) in the Future (Fig. 6). Overall, in the Managed Area, the wet year inundation area was 0.41 % (258 ha) in the Current and changed to 0.53 % (334 ha) in the Future. Similarly, in the dry year, inundation in the Managed Area shifted from 0.09 % (54 ha) to 0.40 % (256 ha) from the Current to the Future case.

4. Discussion

The coupled MIKE SHE–MIKE Hydro model demonstrated robust performance in simulating groundwater level and discharge dynamics across different land-cover types, accurately capturing both seasonal and interannual variability in response to rainfall fluctuations. The low residual water-balance error (<0.2 % of total rainfall) achieved during convergence reflects numerical stability rather than model overfitting, since parameter calibration was constrained by field-measured and literature-supported peat hydraulic properties, and validation against independent datasets confirmed that the close agreement between measured and simulated results arises from realistic process representation. This reliability provides a solid foundation for interpreting the modeled hydrological responses to assess the influence of interannual rainfall variability and land-cover change on water-balance components, the effects of

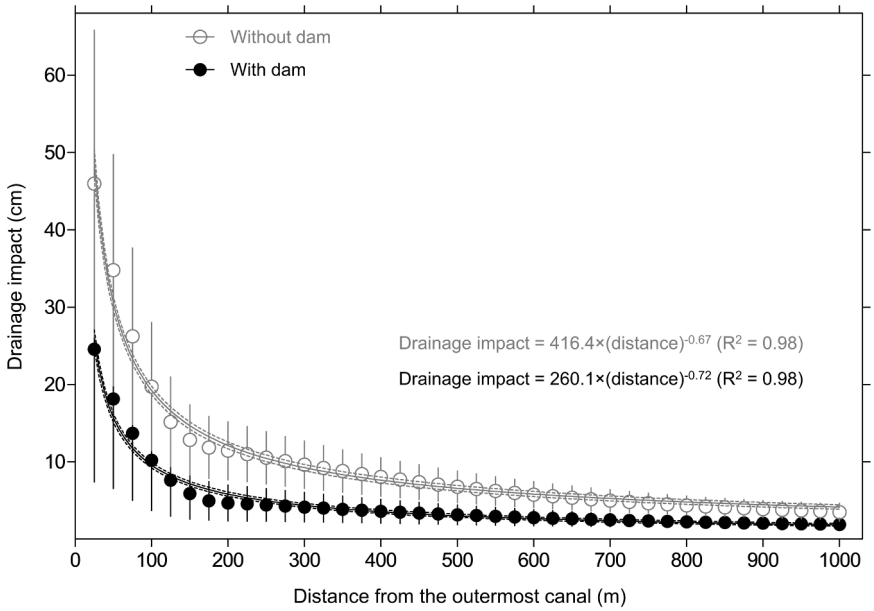

Fig. 4. Drainage impact on groundwater level in adjacent peat swamp forest in Pulau Padang, Riau, Indonesia. The solid line represents the best fit model with 95 % confidence intervals shown as dashed lines. Each point represents the mean groundwater response extracted from 75 model-extracted cross-sections extending from the outermost canals toward the adjacent forest. Vertical bars represent one standard deviation, and all values are derived from model outputs. The analysis uses an average canal depth of 3 m.

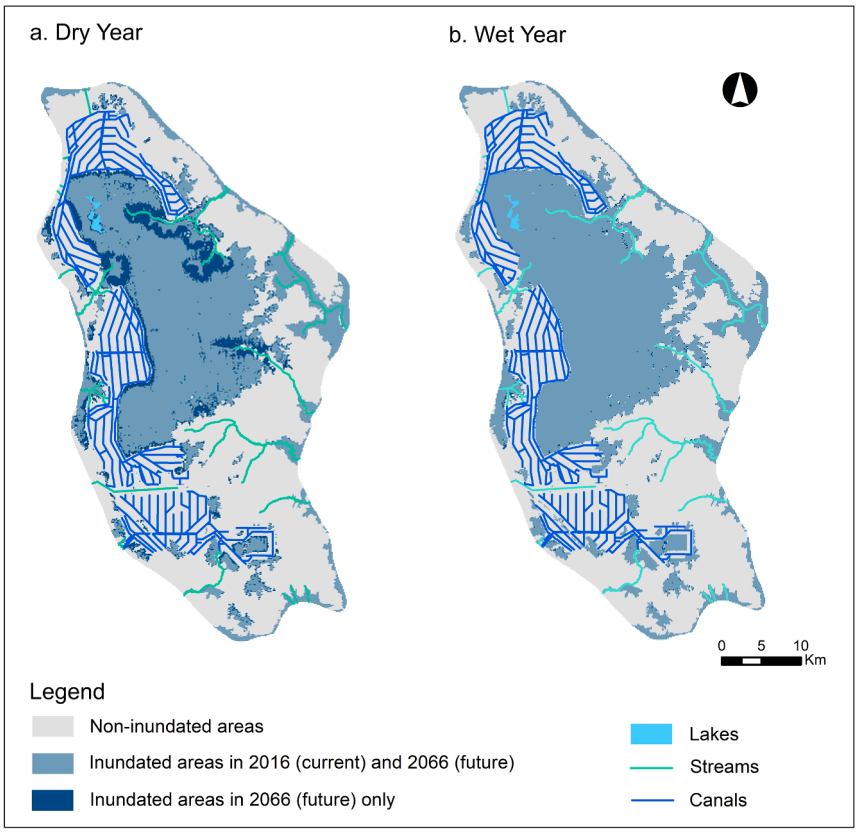

Fig. 5. Modelled inundated area under (a) dry year and (b) wet year for 2016 (Current) and 2066 (Future) in Pulau Padang, Riau, Indonesia. Map show the distribution of areas experiencing inundation depth greater than 1 cm for more than two weeks within the dry and wet years which represent from model outputs. Dark blue color represent the expansion of predicted inundated area in 2066 (Future).

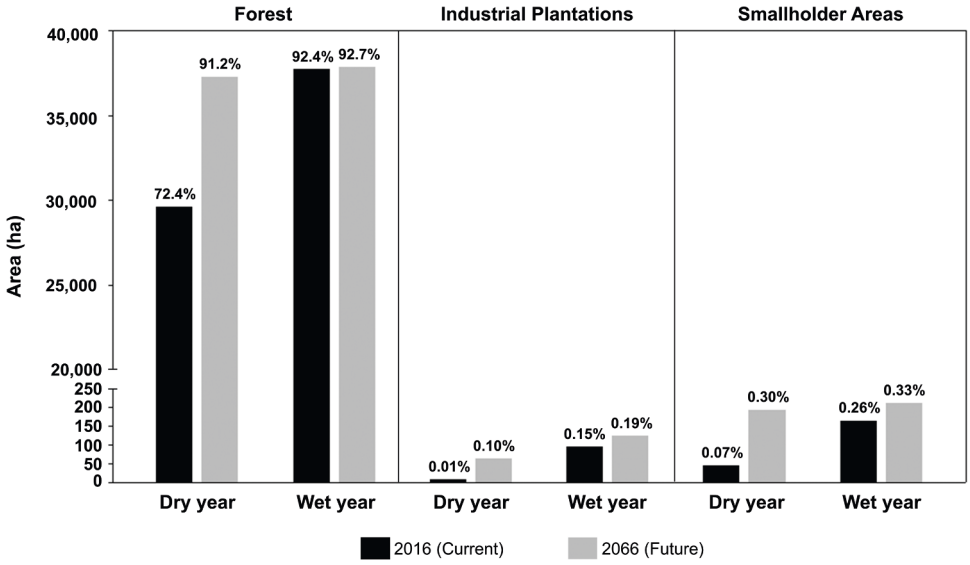

Fig. 6. Modelled inundated area under (a) 2016 (Current) and (b) 2066 (Future) for dry and wet years in Pulau Padang, Riau, Indonesia. Bar charts show the total area experiencing inundation greater than 1 cm for more than two weeks within the year which represent model outputs. Percentages for forests are calculated relative to total forest area, while percentages for smallholder and industrial plantations are calculated relative to total managed area.

water-management control structures, and the projected inundation extent in the context of responsible peatland management.

4.1. Rainfall-driven hydrological variability in tropical peatland

Evapotranspiration represents a primary water loss pathway across both forest and managed areas throughout dry and wet years, with consistently high rates corroborated by field measurements from the tropical peat swamp forests in the region (Hirano et al., 2015; Tang et al., 2019). High canopy rainfall interception coupled with high air temperature (26–28 °C, Deshmukh et al., 2020, 2021, 2023) contributes to intensified evaporation in the dense forest systems (Zimmermann et al., 2013). Additionally, sufficient soil moisture associated with shallow GWLs and high soil temperature (27–28 °C, Deshmukh et al., 2020, 2021, 2023) contribute to high evaporation rates from soil and water surfaces (Ohkubo et al., 2023). Although soil temperature was not directly included as a modeling input in this study, it may have influenced the high evapotranspiration rates which were measured in the field and used to derive the crop factor (Fig. S4). Dense vegetation, combined with high temperatures, soil moisture availability, and ample sun hour throughout the year, further enhances transpiration rates (Hirano et al., 2015; Ohkubo et al., 2023).

Surprisingly, the highest and lowest evapotranspiration did not occur during the wettest and driest years, nor vice versa, suggesting factors beyond rainfall significantly influence evapotranspiration. Specifically, the year 2016, with lower relative humidity and significantly higher net radiation ($p < 0.05$) together with sufficient water availability, produced higher evapotranspiration compared to the wet year 2017 (Fig. S8; Table 2). In contrast, although the year 2018 had higher relative humidity and lower net radiation than the dry year 2015, these differences were not statistically significant ($p > 0.05$). Nevertheless, evapotranspiration remained lower in 2018 than in 2015, indicating that evapotranspiration was influenced by the combined effects of atmospheric demand and water availability rather than by water availability alone. (Deshmukh et al., 2020, 2021; Kosugi et al., 2012; Kume et al., 2010; Mohan and Arumugam, 1996).

Runoff and storage in both forest and managed areas show pronounced seasonal variability driven by rainfall patterns. Under most conditions, groundwater level change (ΔGWL) and total storage change (ΔS) are closely linked because shallow groundwater contributes substantially to total water storage, and changes in rainfall and evapotranspiration typically affect groundwater and near surface storage in the same direction. This coupling reflects the strong hydraulic connection between the saturated and unsaturated zones in tropical peat, where water movement through the upper peat profile responds rapidly to variations in rainfall inputs. However, a clear asynchrony between ΔGWL and ΔS was observed in 2018, which highlights that rainfall variability can influence different storage components at different rates. In early to mid 2018, rainfall decreased after the wet conditions of 2017, which caused rapid depletion of near surface storage through evapotranspiration and peat moisture redistribution, while the deeper saturated zone responded more slowly. This produced a period when ΔS became strongly negative while ΔGWL declined at a slower rate. By mid to late 2018, rainfall increased during the wet season and the upper peat, which has high specific yield (Ismail et al., 2021) and high saturated hydraulic conductivity (Kelly et al., 2014; Kurnianto et al., 2018), responded quickly to the renewed recharge, resulting in positive ΔGWL. Surface water storage, however, continued to decrease because channels, shallow depressions, and near surface layers drained slowly under limited hydraulic gradients. As a result, ΔStorage remained negative even when ΔGWL became positive, creating a short phase lag between groundwater recovery and the slower adjustment of surface and near surface storage components. Future model refinement incorporating vertically varying specific yield and unsaturated-zone hydraulic conductivity is expected to better capture these short-term dynamics and reduce the observed phase lag.

During wet periods, rainfall often exceeds evapotranspiration, leading to increased storage with shallower GWL and increased runoff in both systems. In forest, the GWL elevates near or above the peat surface, allowing overland storage to significantly contribute to total storage change (Fig. S9c) and making surface flow a primary runoff component (Fig. S9c). However, the complex root structures, dense vegetation, and hummock-hollow microtopography (as considered in higher detention storage and Manning's roughness in this study) in the forest suppress the runoff with a relatively longer stream lag time (Dommain et al., 2010; Rezanezhad et al., 2016; Shimamura and Momose, 2007). In contrast, managed peatlands with high canal density and water management practices maintain the GWL below the surface (Fig. S9d). GWL below the surface generates only subsurface flow and making it the predominant runoff component in both wet and dry periods (Fig. S9d; Hooijer et al., 2012; Wösten et al., 2006). The combination of steep hydraulic gradients between canals and adjacent fields and reduced surface roughness (associated with altered vegetation and reduced microtopography) drive significant and rapid subsurface flow (Baird et al., 2017; Holden et al., 2004, 2008), even in deeper peat layers where hydraulic conductivity is up to an order of magnitude lower as observed in Pulau Padang (Table 1) and the Peruvian Amazon forests (Kelly et al., 2014).

During dry periods, declining rainfall inputs with sustained high evapotranspiration demands lead to a reduced runoff, decreased storage, and lower GWL in both systems (Fig. 2). In the forest, the decreased storage and lowered GWL reduces hydraulic gradients between rivers and adjacent forests, thus limiting surface and upper-layer subsurface flow. Therefore, only minor subsurface flow within deeper peat layers contributes to small total runoff. Meanwhile, water control infrastructure in managed area reduces hydraulic gradients between fields and canals, generating low runoff and a stable storage.

The modeled results highlight the hydrological confinement of Pulau Padang's peat system, consistent with its geological setting where the peat layer overlies a marine clay substrate with very low hydraulic conductivity (Cobb et al., 2017; Dommain et al., 2010; Wösten et al., 2006). The simulations indicate that rainfall is primarily partitioned into evapotranspiration and lateral flow, while vertical percolation into the underlying clay layer is negligible. This suggests that all recharge and discharge processes are confined within the peat column, where groundwater recharge represents vertical redistribution between the unsaturated and saturated zones rather than deep aquifer flow. Consequently, rainfall and runoff, with relatively stable evapotranspiration, dominate the island-scale water balance, as reflected by large GWL and storage fluctuations driven by rainfall variability and minimal influence from deeper flow

pathways.

Similar rainfall-driven variability has been reported across the region. Marhaento et al. (2018) showed that both land-use and climate changes significantly altered hydrological processes in a mineral upland catchment in Java, Indonesia, where steep gradients promote rapid runoff generation. In contrast, our simulations for a low gradient peatland with high storage capacity indicate that rainfall variability exerts a much stronger short-term influence on hydrological dynamics than the land cover differences present during the study period. Field observations from Ismail et al. (2021) on Pulau Padang support this conclusion, showing that rainfall and drainage proximity, rather than land-cover type, primarily control GWL fluctuations. Similarly, Treby et al. (2025) reported stable evapotranspiration despite large seasonal rainfall variations in a drained peat swamp forest of Central Kalimantan. In our model, the difference between the very dry 2015 El Niño year and the wetter 2017–2018 period produced relatively constant evapotranspiration across years, meaning that runoff and storage change were the components most strongly affected by rainfall variability. Runoff varied up to eightfold between dry and wet years, and storage change shifted by more than 120 mm, reflecting the large hydrological response to differences in rainfall input. These values represent the upper range of rainfall driven variability associated with a strong ENSO–IOD event and should therefore be interpreted as high end contrasts rather than typical interannual differences. By comparison, the hydrological differences between past peat forest and the current managed land cover, which has been stable for more than a decade, were small, with evapotranspiration differing by only about 1 % and runoff by approximately 6 %. Collectively, these results confirm that rainfall variability dominates short-term hydrological dynamics in tropical peatlands, whereas land-cover differences contribute only minor adjustments to the water balance.

4.2. Impact of land-cover changes on water balance components

To understand why land-cover change produced only small shifts in evapotranspiration, runoff, and storage, we examine the underlying biophysical and hydrological mechanisms. The slightly lower evapotranspiration after land-cover change from forest into managed peatlands is primarily due to reduced plant area index (Table 1), which decreases transpiration (Röll et al., 2019) and reduced canopy interception, consequently reducing evaporation (He et al., 2014). However, the deep-rooted vegetation in managed areas (Table 1) allows access to moisture in the lower peat layers, which can enhance transpiration (Christina et al., 2017; Iida et al., 2016). These contrary effects may jointly lead to only minor differences in overall evapotranspiration between managed and forest peatlands. The reduced surface roughness and microtopography (Table 1) combined with high canal density promotes runoff in managed peatlands in the wet periods. Those changes also result in enhanced runoff velocity and leading to increased subsurface flow into canals, driven by steeper hydraulic gradients and decreased water detention storage. However, the water management infrastructures in managed areas maintain a certain range of GWL, which minimize the storage change.

Although rising temperatures globally are anticipated to increase evapotranspiration (Xu et al., 2021), especially in humid regions (Dezsi et al., 2018; Nooni et al., 2021), our results from Future case suggest minor change in evapotranspiration in these equatorial tropical peatlands, even during dry years like 2015. It seems that evapotranspiration responses may vary spatially with local rainfall and soil moisture dynamics (Dadap et al., 2021). Different subsidence rates in the future for forest and managed peatlands, with higher subsidence rates in managed peatlands relative to forested area, may increase hydraulic gradients across the landscape, which elevates runoff (Table 3). Additionally, expected reduced peat volume due to subsidence rates and sea level rise may further reduce storage capacity in coastal areas by increasing GWL (Liu et al., 2020), which could result in increased runoff even if rainfall levels remain within the Current variability (Table 3, Nuttle and Portnoy, 1992). Importantly, severe and extended drought during climate anomalies such as El Niño and positive IOD events exacerbate these dynamics by intensifying GWL declines due to sustained evapotranspiration, drawdowns reaching up to 59 cm even in the forest areas (Fig. 3; Fig. S7). Our findings underscore peatland vulnerability to prolonged, intense, and frequent dry periods in current and future (Deshmukh et al., 2021, 2023; Garcin et al., 2022; Swails et al., 2018).

Overall, the model results indicate that interannual rainfall variability shows a stronger influence on water balance components than land cover change. The relatively small water balance impact between peat forest in the Past and the managed landscape in the Current reflect the dominance of evapotranspiration in the island's water balance. Evapotranspiration accounts for more than 60 % of annual rainfall, and our results show that ET remains similar between peat swamp forest and Acacia plantations because both systems experience high evaporative demand throughout the year, maintain shallow groundwater levels, and have vegetation with deep rooting access to moisture. Since the primary water loss flux remains nearly unchanged following forest to plantation conversion, the remaining components of the water balance are governed mainly by rainfall variability. This explains why runoff and storage responded strongly to interannual climate differences, particularly between the dry 2015 El Niño year and the La Niña wet 2017 period, while land cover conversion produced only minor adjustments to the overall water balance. Importantly, although the comparison between Past and Future spans nearly a century of contrasting land-cover configurations and incorporates cumulative ground elevation lowering due to peat subsidence, all simulations were conducted under the same range of interannual rainfall variability. This design isolates the structural hydrological effects of land cover and elevation change, demonstrating that even across this counterfactual land-cover trajectory, the magnitude of hydrological change remains small relative to fluctuations driven by interannual rainfall variability.

4.3. Responsible peatland management

Our analysis indicates the importance of dams as a part of water management infrastructures in the managed areas, with lower runoff, and less storage depletion compared to without dams. It seems that the dams in managed areas help to minimize the hydraulic gradients between canals and adjacent field, resulting in lower runoff and less storage depletion. Importantly in the absence of dams in

water management infrastructures, the drainage impact extends farther into adjacent forest areas, emphasizing the role of dams in controlling hydrological conditions beyond canal boundaries. These results indicate that dam placement and maintenance along outermost canals should be considered, as they play a critical role in reducing off-site drainage impacts on adjacent peat swamp forests.

Previous studies have sometimes considered peatland hydrology based on land-use and associated canal presence alone (Wösten and Ritzema, 2001). However, substantial variation of water management practices within the same land-use types, including canal density, dimensions, and groundwater regulation, critically affect hydrological conditions. For instance, increased canal density within a single land-cover type has been linked to higher subsidence rates (Dadap et al., 2021), yet canal density alone cannot fully capture the extent of water management practices. Our results demonstrate that active regulation of water levels through canal and dam operation plays a role that is at least as important as the physical presence of canals, particularly in controlling hydraulic gradients and moderating runoff and storage responses across wet and dry periods. This finding highlights that responsible peatland management should prioritize how water management infrastructure is operated and maintained over time, rather than relying solely on static land-cover or canal-density metrics. Integrating operational rules for canal and dam management into peatland planning frameworks is therefore essential for effective groundwater control and minimizing off-site hydrological impacts, emphasizing the need for site-specific and adaptive management rather than generalized land-cover classifications.

Peat swamp forests exhibit stable water balances across Past, Current, and Future cases, underscoring their resilience to land-cover changes in surrounding areas (Loisel and Gallego-Sala, 2022). Inundation is primarily concentrated in these forest areas, due to their inherent water retention capacity enabled by dense vegetation and complex root structures, which slow water movement and enhance retention (Dommain et al., 2010; Shimamura and Momose, 2007). Additionally, the unique microtopography of forests, featuring hummocks and hollows, enhances water storage by modulating overland flow - hummocks impede water flow, while hollows act as natural reservoirs (Apers et al., 2022). These findings reinforce the importance of conserving large, contiguous peat swamp forest blocks to maintain landscape-scale hydrological buffering capacity. In contrast, smaller or fragmented forest patches may be more vulnerable to hydrological alteration (Cobb et al., 2017).

In this study, inundation extent was defined as surface water depths exceeding 1 cm that persisted for more than two weeks cumulatively within a given year, a criterion intended to capture sustained soil saturation rather than flood disaster conditions (Hein et al., 2022, Sandi et al., 2019). Model simulations show that inundation in managed peatlands on Pulau Padang remained limited (<1 % of the total Managed Area), because industrial plantations occupy the upper portions of the landscape (>4 masl). These higher positions and gentle slopes reduce exposure to tidal and riverine flooding, confining inundation primarily to canal margins and isolated depressions. Controlled drainage through canals and dams further stabilizes groundwater levels and facilitates rapid removal of excess surface water, consistent with drainage behavior observed in other engineered peatland systems (Holden et al., 2004, Evans et al., 2022). This suggests that elevation should be explicitly considered when prioritizing areas for drainage control, restoration, or rewetting interventions. By 2066, projected peat subsidence is estimated to lower ground elevations by approximately ~120 cm in managed areas, which increases local susceptibility to inundation, although the broader topographic structure of the landscape continues to offer protection. These results highlight the need for long-term monitoring of subsidence rates, GWL, and the frequency and duration of inundation to anticipate future hydrological risks and guide adaptive management.

Acute flooding during wet seasons, associated with short-term high-intensity rainfall events is (~300 mm month^{-1}), contrast with chronic inundation risk under Future case driven by continued subsidence and reduced hydraulic gradients, potentially exacerbated by sea-level rise (Kulp and Strauss, 2016; Sweet and Park, 2014). Differentiating between short-term rainfall-driven flooding and longer-term inundation linked to landscape change is critical for designing ydrological risk assessments in responsible peatland management frameworks, which are essential for the development of effective mitigation strategies to protect both ecosystems and local communities (Lupascu et al., 2020). Land-use planning should prioritize regions identified by the model as being sensitive to subsidence- and sea-level-rise-driven inundation, in order to support ecosystem rehabilitation and community adaptation through targeted intervention, monitoring and adaptive management (Clarke and Rieley, 2019). More accurate inundation estimates across diverse climate scenarios could be achieved through comprehensive hydrological modeling, accounting for topographic, hydrological, and climatological factors. This is particularly vital in tropical peatlands, where limited hydrological data often constrain predictive accuracy (Loisel et al., 2020).

This study advances tropical peatland hydrological research by integrating land-cover changes, associated long-term ground elevation lowering due to peat subsidence, interannual rainfall variability, and water-management infrastructure within a physically process-based modelling framework. Few previous studies have quantitatively evaluated the combined influence of these drivers on water-balance components and inundation extent across past, current, and future conditions at the scale of an entire peat-dominated island, while explicitly accounting for spatial variability in vegetation and peat properties. By separating climate-driven and management-driven controls on hydrology, our results provide a clear basis for translating model outputs into operational management decisions related to infrastructure operation and maintenance, monitoring priorities, and spatial targeting of management intervention. The evaluation of water-management control structure in managed areas and adjacent peat swamp forest further provides process-based evidence to support responsible tropical peatland management. Overall, this integrative approach provides new process-level insights into hydrological functioning in tropical peatland mosaics, particularly in regions experiencing strong climate variability and long-term ground elevation change.

From a broader management perspective, while the magnitudes of simulated evapotranspiration, runoff, storage change, and inundation extent reported here are specific to Pulau Padang, several process-level relationships identified in this study are transferable to other lowland ombrotrophic tropical peatland systems with comparable hydrogeomorphic and climatic settings. In particular, the dominance of interannual rainfall variability over incremental land-cover change in controlling runoff and storage change reflects the high sensitivity of shallow peat groundwater systems to climate variability influenced by ENSO and the Indian

Ocean Dipole. In such system, rainfall anomalies translate directly into changes peat water storage which is highly correlated with GWL dynamics. The cumulative influence of peat subsidence on hydraulic gradients and the localized but effective influence of drainage control structures on GWL dynamics, further represents process-level behavior likely applicable across mosaics tropical peatlands under responsible management. By contrast, the limited inundation extent simulated for managed areas in Pulau Padang is site-specific, as it reflects their relatively higher ground elevation within the landscape and the island's coastal configuration, rather than an inherent resistance of managed peatlands to sustained inundation. In landscapes where managed areas occupy lower elevations or experience stronger tidal or fluvial backwater effects, inundation responses may therefore differ substantially. Transferability of the findings therefore lies in these processes' mechanism, rather than in the specific magnitudes reported for Pulau Padang.

4.4. Model limitations and future research outlook

Despite the good performance of the coupled MIKE SHE and MIKE Hydro model in reproducing groundwater levels and discharge, several limitations should be considered when interpreting long term implications. The rainfall period used in the simulations (2015–2018) captured a pronounced rainfall contrast, with 2015 representing a hydrological dry year associated with a strong El Niño and positive IOD (Sulaiman et al., 2023; Supari et al., 2018). Annual rainfall of Pulau Padang in 2015 (~1500 mm) was consistent with nearby BMKG stations in Batam (1563 mm) reflecting the same regional drought pattern, which was also observed at a nearby site in the Kampar Peninsula approximately 120 km away (1291 mm for 295 days in 2012/2013; Yupi et al., 2016). This extreme low rainfall is consistent with the widespread and intense fires that occurred across Indonesia during the strong El Niño combined with a positive IOD event in 2015 (Fanin and van der Werf, 2017; Huijnen et al., 2016; Wooster et al., 2018). As expected, our model results showed significant storage depletion and lower groundwater levels in 2015 compared with the subsequent wetter years, and these patterns align with Sulaiman et al. (2023), who reported groundwater level declines of 1–1.5 m in Central Kalimantan peat forests during the combined El Niño and positive IOD. Together, these results indicate that the pronounced differences in runoff and storage between 2015 and 2017–2018 reflect genuine interannual variability driven by regional climate anomalies rather than measurement bias, although extending the observation period would further enhance statistical confidence in long-term hydrological assessments.

The same meteorological dataset (2014–2018) was used identically across all model cases (Past, Current, and Future), such that differences among cases arise from changes in land cover types, peat ground elevation, and sea-level rise as the boundary conditions rather than from altered climate forcing. We also analysed CMIP6 ensemble rainfall projections for the 2060 s and show that the observed monthly rainfall variability lies within the envelope of projected future rainfall conditions, indicating that this period provides a reasonable representation of regional interannual variability under both Current and Future cases. Nevertheless, the model does not explicitly simulate decadal-scale climate change, long-term shifts in rainfall seasonality, or changes in rainfall intensity, and the Future simulations should therefore be interpreted as process-based hydrological sensitivity analysis rather than deterministic climate projections. Incorporating fully dynamic climate projections in future modelling studies would allow explicit assessment of these effects.

The 2066 case retained the 2016 land cover spatial distribution and is explicitly treated as a policy-compliance scenario, consistent with Indonesia's peat protection policies (Presidential Decree No. 8 of 2015), rather than as a deterministic projection of land-use condition over a 50-year projection. This Future case was designed to isolate hydrological responses to cumulative peat subsidence, sea-level rise and rainfall variability under stable land management, thereby representing one plausible management pathway instead of a comprehensive exploration of alternative land-use futures. However, alternative trajectories involving unplanned deforestation or uncontrolled land use change (Anand and Oinam, 2020, Chimner et al., 2017, Sumarga et al., 2016, Sutton et al., 2024, Tahir et al., 2025) may alter hydrological functioning by increasing drainage density, weakening or removing dam canals as water-management structures, accelerating peat subsidence, and reducing surface storage capacity. Under such trajectories, hydrological responses such as increased runoff, deeper groundwater drawdown, and chronic inundation would likely be amplified relative to the case presented here. Our model therefore provides a conditional baseline assessment under continued policy compliance, and future scenario work should include land-use uncertainty to capture this potential impact. Associated peat physical and hydraulic properties for each land-cover types were parameterized using field data and literature values and held constant across model years, although peat properties are also influenced by drainage density (Lennartz and Liu, 2019), decomposition stage (Morris et al., 2015), and disturbance history (Wahyono et al., 2023). The model does not represent feedbacks between peat oxidation, subsidence, and changing peat physical and hydraulic properties, which may further influence long-term runoff and inundation patterns. Similarly, vegetation parameters, such as LAI, were kept static despite variation associated with plantation age or seasonal dynamics; incorporating remote sensing products such as LAI time series could improve future model setup (Li et al., 2025, Liu et al., 2012).

5. Conclusions

MIKE SHE-MIKE Hydro framework is a physically based distributed and deterministic hydrological model that integrates rainfall, evapotranspiration, runoff, and water storage dynamics across surface and subsurface components. The research work undertaken here has in fact used advanced and refined modules available and has constructed a very complex and extensive data set in a sizable tropical peatland landscape setting. Results highlight that interannual rainfall variability, primarily driven by ENSO and IOD events, have a more pronounced influence on runoff and storage changes compared to land-cover configuration alone. Forested peatlands affirm the higher hydrological resilience, which sustain their hydrological balance despite changes in surrounding land cover. However, these ecosystems remain susceptible to climate anomalies, such as El Niño and positive IOD events, which induce significant GWL declines during prolonged and frequent droughts.

All simulation cases were conducted under an identical range of interannual rainfall variability, thus the reported difference isolate the structural effect of land cover, peat ground elevation, and water management, rather than representing historical or future climate trajectories. Modeled land-cover conversion from peat forest to managed areas resulted in only minor differences in evapotranspiration (~1 %) and runoff (~6 %) under identical rainfall conditions. Further, dams in the managed peatland effectively limit drainage impacts within 300 m of outermost canals to neighboring ecosystems. These infrastructures regulate GWL dynamics by minimizing runoff and hydraulic gradients in the dry periods and facilitating drainage of surplus water to minimize inundation in the wet periods. Inundation modeling further demonstrates that managed peatlands located on higher elevation of the landscape experience minimal surface inundation (<1 % of the total managed areas), suggesting favorable long-term management conditions from a hydrological perspective, with potential implications for economic sustainability. However, these outcomes remain conditional on continued land-use policy enforcement and active water management, and alternative future trajectories could produce different hydrological responses. These findings emphasize the necessity of integrating topographic, hydrological, and climatological data within comprehensive modeling frameworks to support spatial prioritization of intervention, long-term monitoring of peat subsidence and GWL dynamics, and adaptive management strategies that account both climate variability and landscape change.

This study establishes a robust hydrological modelling framework for science-based peatland management strategies that address the interplay of land-cover changes, water management practices, and climate variability. Extending this framework to other tropical peatlands, such as those in the Amazon and Congo basins, offers a pathway to broadening our understanding of diverse peatland hydrology. Furthermore, integrating this model with carbon and greenhouse gas emission analyses could provide a comprehensive assessment of land-use and climate impacts on tropical peatland ecosystem services. These insights will enhance conservation and restoration efforts, advancing responsible peatland management at regional and global scales.

Author statement

We are submitting a revised version of our manuscript titled **"Hydrological Dynamics in a Tropical Peatland Mosaic: Influence of Land-Cover Changes and Rainfall Variability."** This revision addresses all reviewer comments in detail, and all changes are documented in the "Response to Reviewers" file and in the annotated manuscript. The manuscript is original, has not been published elsewhere, and is not under consideration by any other journal.

Declaration of Competing Interest

The authors declare that they have no known competing financial interests or personal relationships that could have appeared to influence the work reported in this paper

Acknowledgements

The authors thank Asia Pacific Resources International Ltd (APRIL) for providing financial and logistic support. The contributions of CE, SP, DA, FA, and SS form part of their role to the Independent Peat Expert Working Group (IPEWG), which was set up by APRIL to provide objective science-based advice on peatland management. The authors also acknowledge the extended support from DHI Water and Environment, Singapore & Denmark offices for hydrological modeling aspects. This paper is a contribution to the League of geophysical research eXcellences for tropical Asia (LeXtra).

Appendix A. Supporting information

Supplementary data associated with this article can be found in the online version at doi:10.1016/j.ejrh.2026.103185.

Data availability

Data will be made available on request.

References

Abbott, M.B., Bathurst, J.C., Cunge, J.A., O'Connell, P.E., Rasmussen, J., 1986. An introduction to the European hydrological system – systeme hydrologique Europeen, "SHE", 2: structure of a physically-based, distributed modelling system. J. Hydrol. 87 (1), 61–77. https://doi.org/10.1016/0022-1694(86)90115-0.

Allen, R.G., Pereira, L.S., Raes, D., Smith, M., 1998. Crop evapotranspiration: Guidelines for computing crop water requirements (FAO Irrigation and Drainage Paper No. 56). FAO.

Alsepan, G., Minobe, S., 2020. Relations between interannual variability of regional-scale Indonesian precipitation and large-scale climate modes during 1960-2007. J. Clim. 33 (12), 5271–5291. https://doi.org/10.1175/JCLI-D-19-0811.1.

Amirudin, A.A., Salimun, E., Tangang, F., Juneng, L., Zuhairi, M., 2020. Differential Influences of Teleconnections from the Indian and Pacific Oceans on Rainfall Variability in Southeast Asia. Atmosphere 11 (9), 886. https://doi.org/10.3390/atmos11090886.

Anand, V., Oinam, B., 2020. Future land use land cover prediction with special emphasis on urbanization and wetlands. Remote Sens. Lett. 11 (3), 225–234. https://doi.org/10.1080/2150704X.2019.1704304.

Anshari, G.Z., Afifudin, M., Nuriman, M., Gusmayanti, E., Arianie, L., Susana, R., Nusantara, R.W., Sugardjito, J., Rafiastanto, A., 2010. Drainage and land use impacts on changes in selected peat properties and peat degradation in West Kalimantan Province, Indonesia. Biogeoscience 7, 3403–3419. https://doi.org/10.5194/bg-7-3403-2010.

Apers, S., De Lannoy, G.J.M., Baird, A.J., Cobb, A.R., Dargie, G.C., del Aguila Pasquel, J., Gruber, A., Hastie, A., Hidayat, H., Hirano, T., Hoyt, A.M., Jovani-Sancho, A. J., Katimon, A., Kurnain, A., Koster, R.D., Lampela, M., Mahanama, S.P.P., Melling, L., Page, S.E., Reichle, R.H., Taufik, M., Vanderborght, J., Bechtold, M., 2022. Tropical Peatland Hydrology simulated with a global land surface model. J. Adv. Model. Earth Syst. 14 (3). https://doi.org/10.1029/2021MS002784.

Arcement, G.J., & Schneider, V.R. (1989). Guide for selecting Manning's roughness coefficients for natural channels and flood plains (Water Supply Paper 2339). U.S. Geological Survey. https://doi.org/10.3133/wsp2339.

Baird, A.J., Low, R., Young, D., Swindles, G.T., Lopez, O.R., Page, S., 2017. High permeability explains the vulnerability of the carbon store in drained tropical peatlands. Geophys. Res. Lett. 44 (3), 1333–1339. https://doi.org/10.1002/2016GL072245.

Beckwith, C.W., Baird, A.J., Heathwaite, A.L., 2003. Anisotropy and depth-related heterogeneity of hydraulic conductivity in a bog peat. I: laboratory measurements. Hydrol. Process. 17 (1), 89–101. https://doi.org/10.1002/hyp.1116.

Bouwer, H., Rice, R.C., 1976. A slug test for determining hydraulic conductivity of unconfined aquifers with completely or partially penetrating wells. Water Resour. Res. 12 (3), 423–428. https://doi.org/10.1029/WR012i003p00423.

Brady, M.A. (1997). Organic matter dynamics of coastal peat deposits in Sumatra (Ph.D. Thesis). University of British Columbia, Vancouver, Canada. https://doi.org/10.14288/1.0075286.

Chimner, R.A., Cooper, D.J., Wurster, F.C., Rochefort, L., 2017. Multi-decadal changes in water table levels alter peatland carbon cycling. Ecosystems 20 (5), 1042–1057. https://doi.org/10.1007/s10021-016-0085-3.

Christina, M., Nouvellon, Y., Laclau, J., Stape, J., Bouillet, J., Lambais, G., Maire, G., 2017. Importance of deep water uptake in tropical eucalypt forest. Funct. Ecol. 31, 509–519. https://doi.org/10.1111/1365-2435.12727.

Church, J.A., Clark, P.U., Cazenave, A., Gregory, J.M., Jevrejeva, S., Levermann, A., Merrifield, M.A., Milne, G.A., Nerem, R.S., Nunn, P.D., Payne, A.J., Pfeffer, W.T., Stammer, D., Unnikrishnan, A.S., 2013. Sea-level rise by 2100. -1445 Science 342 (6165), 1445. https://doi.org/10.1126/science.342.6165.1445-a.

Clarke, D., Rieley, J.O., 2019. Strategy for Responsible Peatland Management, 6th ed. International Peatland Society, Jyväskylä, Finland.

Cobb, A.R., Hoyt, A.M., Gandois, L., Eri, J., Dommain, R., Salim, K.A., Kai, F.M., Su'ut, N.S.H., Harvey, C.F., 2017. How temporal patterns in rainfall determine the geomorphology and carbon fluxes of tropical peatlands. Proc. Natl. Acad. Sci. 114 (26), E5187–E5196. https://doi.org/10.1073/pnas.1701090114.

Dadap, N.C., Hoyt, A.M., Cobb, A.R., Oner, D., Kozlnski, M., Fua, P.V., Rao, K., Harvey, C.F., Konings, A.G., 2021. Drainage canals in Southeast Asian Peatlands Increase Carbon Emissions. e2020AV000321 AGU Adv. 2. https://doi.org/10.1029/2020AV000321.

Dai, Z., Li, C., Trettin, C., Sun, G., Amatya, D., Li, H., 2010. Bi-criteria evaluation of the MIKE SHE model for a forested watershed on the South Carolina coastal plain. Hydrol. Earth Syst. Sci. 14 (6), 1033–1046. https://doi.org/10.5194/hess-14-1033-2010.

Deshmukh, C.S., Julius, D., Desai, A.R., Asyhari, A., Page, S.E., Nardi, Susanto, A.P., Nurholis, Hendrizal, M., Kurnianto, S., Suardiwerianto, Y., Agus, F., Astiani, D., Sabiham, S., Gauci, V., Evans, C.D., 2021. Conservation slows down emission increase from a tropical peatland in Indonesia. Curr. Clim. Nat. Geosci. 14, 484–490. https://doi.org/10.1038/s41561-021-00785-2.

Deshmukh, C.S., Julius, D., Evans, C.D., Nardi, Susanto, A.P., Page, S.E., Gauci, V., Lauren, A., Sabiham, S., Agus, F., Asyhari, A., Kurnianto, S., Suardiwerianto, Y., Desai, A.R., 2020. Impact of forest plantation on methane emissions from tropical peatland. Glob. Change Biol. 26 (4), 2477–2495. https://doi.org/10.1111/gcb.15019.

Deshmukh, C.S., Susanto, A.P., Nardi, N., Nurholis, N., Kurnianto, S., Suardiwerianto, Y., Hendrizal, M., Rhinaldy, A., Mahfiz, R.E., Desai, A.R., Page, S.E., Cobb, A.R., Hirano, T., Guérin, F., Serça, D., Prairie, Y.T., Agus, F., Astiani, D., Sabiham, S., Evans, C.D., 2023. Net greenhouse gas balance of fibre wood plantation on peat in Indonesia. Nature 616 (7958), 740–746. https://doi.org/10.1038/s41586-023-05860-9.

Dezsi, Ş., Mîndrescu, M., Petrea, D., Rai, P.K., Hamann, A., Nistor, M.M., 2018. High-resolution projections of evapotranspiration and water availability for Europe under climate change. Int. J. Climatol. 38 (10), 3832–3841. https://doi.org/10.1002/joc.5537.

DHI, 2017a. MIKE SHE user manual: Volume 1 – User guide. Danish Hydraulics Institute, Hørsholm, Denmark.

DHI, 2017b. MIKE Hydro River User Guide. Danish Hydraulics Institute, Hørsholm, Denmark.

Dommain, R., Couwenberg, J., Joosten, H., 2010. Hydrological self-regulation of domed peatlands in Southeast Asia and consequences for conservation and restoration. Mires Peat 6, 1–17.

Dommain, R., Couwenberg, J., Joosten, H., 2011. Development and carbon sequestration of tropical peat domes in South-east Asia: links to post-glacial sea-level changes and Holocene climate variability. Quat. Sci. Rev. 30, 999–1010. https://doi.org/10.1016/j.quascirev.2011.01.018.

Evans, C.D., Irawan, D., Suardiwerianto, Y., Kurnianto, S., Deshmukh, C., Asyhari, A., Page, S., Astiani, D., Agus, F., Sabiham, S., Laurén, A., Williamson, J., 2022. Long-term trajectory and temporal dynamics of tropical peat subsidence in relation to plantation management and climate. Geoderma 428, 116100. https://doi.org/10.1016/j.geoderma.2022.116100.

Evans, C.D., Williamson, J.M., Kacaribu, F., Irawan, D., Suardiwerianto, Y., Hidayat, M.F., Lauren, A., Page, S., 2019. Rates and spatial variability of peat subsidence in Acacia plantation and forest landscapes in Sumatra, Indonesia. Geoderma 338, 410–421. https://doi.org/10.1016/j.geoderma.2018.12.028.

Fanin, T., van der Werf, G.R., 2017. Precipitation–fire linkages in Indonesia (1997–2015). Biogeosciences 14 (18), 3995–4008. https://doi.org/10.5194/bg-14-3995-2017.

Garcin, Y., Schefuß, E., Dargie, G.C., Hawthorne, D., Lawson, I.T., Sebag, D., Biddulph, G.E., Crezee, B., Bocko, Y.E., Ifo, S.A., Wenina, Y.E.M., Mbemba, M., Ewango, C.E.N., Emba, O., Bola, P., Tabu, J.K., Tyrrell, G., Young, D.M., Gassier, G., Lewis, S.L., 2022. Hydroclimatic vulnerability of peat carbon in the central Congo Basin. Nature 612 (7939), 277–282. https://doi.org/10.1038/s41586-022-05389-3.

Gumbricht, T., Roman-Cuesta, R.M., Verchot, L., Herold, M., Wittmann, F., Householder, E., Herold, N., Murdiyarso, D., 2017. An expert system model for mapping tropical wetlands and peatlands reveal South America as the largest contributor. Glob. Change Biol. 23 (9), 3581–3599. https://doi.org/10.1111/gcb.13689.

Hapsari, K.A., Jennerjahn, T., Nugroho, S.H., Yulianto, E., Behling, H., 2022. Sea level rise and climate change acting as interactive stressors on development and dynamics of tropical peatlands in coastal Sumatra and South Borneo since the last glacial maximum. Glob. Change Biol. 28 (10), 3459–3479. https://doi.org/10.1111/gcb.16131.

Hardt, E., Ferraz, S.F.B., Vettorazzi, C.A., Vogt, P., 2018. GIS-based detection and quantification of patch-boundary patterns for identifying landscape mosaics. Appl. Ecol. Environ. Res. 16 (2), 1381–1398. https://doi.org/10.15666/AEER/1602_13811398.

Harrison, M.E., Ottay, J.B., D'Arcy, L.J., Cheyne, S.M., Anggodo, Belcher, C., Cole, L., Dohong, A., Ermiasi, Y., Feldpausch, T., Gallego-Sala, A., Gunawan, A., Höing, A., Husson, S.J., Kulu, I.P., Sorbagio, A.M., Mang, S., Mercado, L., Morrogh-Bernard, H.C., van Veen, F.J.F., 2019. Tropical forest and peatland conservation in Indonesia: Challenges and directions (Early View). People Nat.. https://doi.org/10.1002/pan3.10060.

He, Z.B., Yang, J.J., Du, J., Zhao, W.Z., Liu, H., Chang, X.X., 2014. Spatial variability of canopy interception in a spruce forest of the semiarid mountain regions of China. Agric. For. Meteorol. 188, 58–63. https://doi.org/10.1016/j.agrformet.2013.12.008.

Hein, L., Sumarga, E., Quiñones, M., Suwarno, A., 2022. Effects of soil subsidence on plantation agriculture in Indonesian peatlands. Reg. Environ. Change 22 (4), 121. https://doi.org/10.1007/s10113-022-01979-z.

Henman, J., Poulter, B., 2008. Inundation of freshwater peatlands by sea level rise: Uncertainty and potential carbon cycle feedbacks. J. Geophys. Res. Biogeosciences 113 (G1). https://doi.org/10.1029/2006jg000395.

Hidayat, R., Kizu, S., 2010. Influence of the Madden–Julian Oscillation on Indonesian rainfall variability in austral summer. Int. J. Climatol. 30, 1816–1825. https://doi.org/10.1002/joc.2005.

Hirano, T., Kusin, K., Limin, S., Osaki, M., 2015. Evapotranspiration of tropical peat swamp forests. Glob. Change Biol. 21 (5), 1914–1927. https://doi.org/10.1111/gcb.12653.

Hirano, T., Segah, H., Kusin, K., Limin, S., Takahashi, H., Osaki, M., 2012. Effects of disturbances on the carbon balance of tropical peat swamp forest. Glob. Change Biol. 18 (11), 1–13. https://doi.org/10.1111/j.1365-2486.2012.02793.x.

Holden, J., Chapman, P.J., Labadz, J.C., 2004. Artifical drainage of peatlands: hydrological and hydrochemical process and wetland restoration. Prog. Phys. Geogr. 28 (1), 95–123. https://doi.org/10.1191/0309133304pp403ra.
Holden, J., Kirkby, M.J., Lane, S.N., Milledge, D.G., Brookes, C.J., Holden, V., McDonald, A.T., 2008. Overland flow velocity and roughness properties in peatlands. Water Resour. Res. 44 (6). https://doi.org/10.1029/2007wr006052.
Hooijer, A., 2005. Hydrology of tropical wetland forests: recent research results from Sarawak peatswamps. In: Bonell, M., Bruijnzeel, L.A. (Eds.), Forests, water and people in the humid tropics. Cambridge University Press, pp. 447–461. https://doi.org/10.1017/CBO9780511535666.023.
Hooijer, A., Page, S., Jauhiainen, J., Lee, W.A., Lu, X.X., Idris, A., Anshari, G., 2012. Subsidence and carbon loss in drained tropical peatlands. Biogeoscience 9, 1053–1071. https://doi.org/10.5194/bg-9-1053-2012.
Hoyt, A.M., Chaussard, E., Seppalainen, S.S., Harvey, C.F., 2020. Widespread subsidence and carbon emissions across Southeast Asian Peatlands. Nat. Geosci. 13 (6), 1–6. https://doi.org/10.1038/s41561-020-0575-4.
Huijnen, V., Wooster, M.J., Wooster, M.J., Kaiser, J.W., Gaveau, D.L.A., Flemming, J., Parrington, M., Inness, A., Murdiyarso, D., Murdiyarso, D., Main, B., van Weele, M., 2016. Fire carbon emissions over maritime southeast Asia in 2015 largest since 1997. Sci. Rep. 6 (1), 26886. https://doi.org/10.1038/srep26886.
Iida, S., Shimizu, T., Tamai, K., Kabeya, N., Shimizu, A., Ito, E., Ohnuki, Y., Chann, S., Keth, N., 2016. Interrelationships among dry season leaf fall, leaf flush and transpiration: insights from sap flux measurements in a tropical dry deciduous forest. Ecohydrology 9, 472–486. https://doi.org/10.1002/eco.1650.
Ismail, I., Haghighi, A.T., Marttila, H., Kurniawan, U., Karyanto, O., Klove, B., 2021. Water table variations on different land use units in a drained tropical peatland island of Indonesia. Hydrol. Res. 52 (6), 1373. https://doi.org/10.2166/nh.2021.062.
Kelly, T.J., Baird, A.J., Roucoux, K.H., Baker, T.R., Honorio Coronado, E.N., Ríos, M., Lawson, I.T., 2014. The high hydraulic conductivity of three wooded tropical peat swamps in northeast Peru: measurements and implications for hydrological function. Hydrol. Process. 28 (9), 3373–3387. https://doi.org/10.1002/hyp.9884.
Knoben, W.J., Freer, J.E., Woods, R.A., 2019. Inherent benchmark or not? Comparing Nash–Sutcliffe and Kling–Gupta efficiency scores. Hydrol. Earth Syst. Sci. 23 (10), 4323–4331. https://doi.org/10.5194/hess-23-4323-2019.
Kosugi, Y., Takanashi, S., Tani, M., Ohkubo, S., Matsuo, N., Itoh, M., Noguchi, S., Nik, A., 2012. Effect of inter-annual climate variability on evapotranspiration and canopy CO2 exchange of a tropical rainforest in Peninsular Malaysia. J. For. Res. 17, 227–240. https://doi.org/10.1007/s10310-010-0235-4.
Kulp, S., Strauss, B.H., 2016. Global DEM errors underpredict coastal vulnerability to sea level rise and flooding. Front. Earth Sci. 4, 36. https://doi.org/10.3389/feart.2016.00036.
Kume, T., Tanaka, N., Kuraji, K., Komatsu, H., Yoshifuji, N., Saitoh, T., Suzuki, M., Kumagai, T., 2010. Ten-year evapotranspiration estimates in a Bornean tropical rainforest. Agric. For. Meteorol. 151, 1183–1192. https://doi.org/10.1016/j.agrformet.2011.04.005.
Kurnianto, S., Selker, J., Kauffman, J.B., Murdiyarso, D., Peterson, J.T., 2018. The influence of land cover changes on the variability of conductivity in tropical peatlands. Mitig. Adapt. Strateg. Glob. Change 24 (4), 535–555. https://doi.org/10.1007/s11027-018-9802-3.
Lampela, M., Jauhiainen, J., Kamari, I., Koskinen, M., Tanhuanpaa, T., Valkeapaa, A., Vasander, H., 2016. Ground surface microtopography and vegetation patterns in tropical peat swamp forest. Catena 139, 127–136. https://doi.org/10.1016/j.catena.2015.12.016.
Lennartz, B., Liu, H., 2019. Hydraulic functions of peat soils and ecosystem service. Front. Environ. Sci. 7, 92. https://doi.org/10.3389/fenvs.2019.00092.
Lewis, C., Albertson, J., Xu, X., Kiely, G., 2011. Spatial variability of hydraulic conductivity and bulk density along a blanket peatland hillslope. Hydrol. Process. 26 (10), 1527–1537. https://doi.org/10.1002/hyp.8252.
Li, W., Dickinson, R.E., Fu, R., Niu, G.Y., Yang, Z.L., Canadell, J.G., 2007. Future precipitation changes and their implications for tropical peatlands. Geophys. Res. Lett. 34 (1).
Li, Y., Wang, B., Zhao, X., Zhang, Y., Qiao, L., 2025. Inversion and analysis of leaf area index (LAI) of urban park based on unmanned aerial vehicle (UAV) multispectral remote sensing and random forest (RF). PLOS ONE 20 (3), e0320608. https://doi.org/10.1371/journal.pone.0320608.
Liu, J., Pattey, E., Jégo, G., 2012. Assessment of vegetation indices for regional crop green LAI estimation from Landsat images over multiple growing seasons. Remote Sens. Environ. 123, 347–358. https://doi.org/10.1016/j.rse.2012.04.002.
Liu, H., Price, J., Rezanezhad, F., Lennartz, B., 2020. Centennial-scale shifts in hydrophysical properties of peat induced by drainage. e2020WR027538 Water Resour. Res. 56 (10). https://doi.org/10.1029/2020WR027538.
Loisel, J., Gallego-Sala, A., 2022. Ecological resilience of restored peatlands to climate change. Commun. Earth Environ. 3 (1), 208. https://doi.org/10.1038/s43247-022-00547-x.
Loisel, J., Gallego-Sala, A.V., Amesbury, M.J., Magnan, G., Anshari, G., Beilman, D.W., Benavides, J.C., Blewett, J., Camill, P., Charman, D.J., Chawvhai, S., Hedgpeth, A., Kleinen, T., Korhola, A., Large, D., Mansilla, C.A., Müller, J., van Bellen, S., West, J.B., Wu, J., 2020. Expert assessment of future vulnerability of the global peatland carbon sink. Nat. Clim. Change 11, 70–77. https://doi.org/10.1038/s41558-020-00944-0.
Lupascu, M., Vakkey, H., Tortajada, C., 2020. Is flooding considered a threat in the degraded tropical peatlands? Sci. Total Environ. 723, 137988. https://doi.org/10.1016/j.scitotenv.2020.137988.
Marhaento, H., Booij, M.J., Hoekstra, A.Y., 2018. Hydrological response to future land-use change and climate change in a tropical catchment. Hydrol. Sci. J. 63 (9), 1368–1385. https://doi.org/10.1080/02626667.2018.1511054.
Mbow, H.O.P., Reisinger, A., Canadell, J., O'Brien, P., 2017. Special report on climate change, desertification, land degradation, sustainable land management, food security, and greenhouse gas fluxes in terrestrial ecosystems (SR2). Intergov. Panel Clim. Change (IPCC). ⟨https://archive.ipcc.ch/report/srccl/pdf/sr2_background_report_final.pdf⟩.
Mezbahuddin, M., Grant, R.F., Hirano, T., 2015. How hydrology determines seasonal and interannual variations in water table depth, surface energy exchange, and water stress in a tropical peatland: Modeling versus measurements. J. Geophys. Res. Biogeosciences 120, 2132–2157. https://doi.org/10.1002/2015JG003005.
Mezbahuddin, S., Nikonovas, T., Spessa, A., Grant, R.F., Imron, M.A., Doerr, S.H., Clay, G.D., 2023. Accuracy of tropical peat and non-peat fire forecasts enhanced by simulating hydrology. Sci. Rep. 13 (1), 619. https://doi.org/10.1038/s41598-022-27075-0.
Miettinen, J., Shi, C., Liew, S.C., 2016. Land-cover distribution in the peatlands of Peninsular Malaysia, Sumatra and Borneo in 2015 with changes since 1990. Glob. Ecol. Conserv. 6, 67–78. https://doi.org/10.1016/j.gecco.2016.02.004.
Mohan, S., Arumugam, N., 1996. Relative importance of meteorological variables in evapotranspiration: Factor analysis approach. Water Resour. Manag. 10, 1–20. https://doi.org/10.1007/BF00698808.
Moriasi, D.N., Arnold, J.G., van Liew, M.W., Bingner, R.I., Harmel, R.D., Veith, T.L., 2007. Model evaluation guidelines for systematic quantification of accuracy in watershed simulations. Trans. ASABE 50 (3), 885–900. https://doi.org/10.13031/2013.23153.
Morris, P.J., Baird, A.J., Belyea, L.R., 2015. Bridging the gap between models and measurements of peat hydraulic conductivity. Water Resour. Res. 51, 5353–5364. https://doi.org/10.1002/2015WR017264.
Muhammad, F.R., Lubis, S.W., Setiawan, S., 2020. Impacts of the Madden–Julian oscillation on precipitation extremes in Indonesia. Int. J. Climatol. 41 (3), 1970–1984. https://doi.org/10.1002/joc.6941.
Nishimura, T.B., Suzuki, E., Kohyama, T., Tsuyuzaki, S., 2007. Mortality and growth of trees in peat-swamp and health forests in Central Kalimantan after severe drought. Plant Ecol. 188 (2), 165–177. https://doi.org/10.1007/s11258-006-9154-z.
Nooni, I.K., Hagan, D.F., Wang, G., Ullah, W., Lu, J., Li, S., Dzakpasu, M., Prempeh, N.A., Lim Kam Sian, K.T., 2021. Future changes in simulated evapotranspiration across Continental Africa based on CMIP6 CNRM-CM6. Int. J. Environ. Res. Public Health 18 (13), 6760. https://doi.org/10.3390/ijerph18136760.
Nuttle, W.K., Portnoy, J.W., 1992. Effect of rising sea level on runoff and groundwater discharge to coastal ecosystems. Estuar. Coast. Shelf Sci. 34 (2), 203–212. https://doi.org/10.1016/s0272-7714(05)80106-4.
Ohkubo, S., Hirano, T., Kusin, K., 2023. Influence of disturbance on transpiration and evaporation in tropical peat swamp forests. J. Hydrol. 620, 129523. https://doi.org/10.1016/j.jhydrol.2023.129523.
Page, S., Mishra, S., Agus, F., et al., 2022. Anthropogenic impacts on lowland tropical peatland biogeochemistry. Nat. Rev. Earth Environ. 3, 426–443. https://doi.org/10.1038/s43017-022-00289-6.

Page, S.E., Rieley, J.O., Banks, C.J., 2011. Global and regional importance of the tropical peatland carbon pool. Glob. Change Biol. 17 (2), 798–818. https://doi.org/10.1111/j.1365-2486.2010.02279.x.
Putra, S.S., Baird, A.J., Holden, J., 2022. Modelling the performance of bunds and ditch dams in the hydrological restoration of tropical peatlands. Hydrol. Process. 36 (1), e14470. https://doi.org/10.1002/hyp.14470.
Putra, S.S., Holden, J., Baird, A.J., 2021. The effects of ditch dams on water-level dynamics in tropical peatlands. Hydrol. Process. 35 (5), e14174. https://doi.org/10.1002/hyp.14174.
Rahim, B.E.A., Yusoff, I., Jafri, A.M., Othman, Z., Ghani, A.A., 2012. Application of MIKE SHE modelling system to set up a detailed water balance computation. Water Environ. J. 26 (4), 490–503. https://doi.org/10.1111/j.1747-6593.2012.00309.x.
Refsgaard, J.C., 1997. Parameterisation, calibration and validation of distributed hydrological models. J. Hydrol. 198 (1-4), 69–97. https://doi.org/10.1016/S0022-1694(96)03329-X.
Rezanezhad, F., Price, J.S., Quinton, W.L., Lennartz, B., Milojevic, T., van Cappelen, P., 2016. Structure of peat soils and implications for water storage, flow and solute transport: a review update for geochemists. Chem. Geol. 428, 75–84. https://doi.org/10.1016/j.chemgeo.2016.03.010.
Röll, A., Niu, F., Meijide, A., Ahongshangbam, J., Ehbrecht, M., Guillaume, T., Gunawan, D., Hardanto, A., Hendrayanto, Hertel, D., Kotowska, M.M., Kreft, H., Kuzyakov, Y., Leuschner, C., Nomura, M., Polle, A., Rembold, K., Sahner, J., Seidel, D., Hölscher, D., 2019. Transpiration on the rebound in lowland Sumatra. Agric. For. Meteorol. 274, 160–171. https://doi.org/10.1016/j.agrformet.2019.04.017.
Saji, N.H., Goswami, B.N., Vinayachandran, P.N., Yamagata, T., 1999. A dipole mode in the tropical Indian Ocean. Nature 401 (6751), 360–363. https://doi.org/10.1038/43854.
Sandi, S.G., Saco, P.M., Saintilan, N., Wen, L., Riccardi, G., Kuczera, G., Willgoose, G., Rodríguez, J.F., 2019. Detecting inundation thresholds for dryland wetland vulnerability. Adv. Water Resour. 128, 168–182. https://doi.org/10.1016/j.advwatres.2019.04.016.
Shimamura, T., Momose, K., 2007. Reciprocal interactions between carbon storage function and plant species diversity in a tropical peat swamp forest. Asian Afr. Area Stud. 6 (2), 279–296. https://doi.org/10.14956/asafas.6.279.
Sulaiman, A., Osaki, M., Takahashi, H., Yamanaka, M.D., Susanto, R.D., Shimada, S., Kimura, K., Hirano, T., Wetadewi, R.I., Sisva, S., Kato, T., Kozan, O., Kubo, H., Awaluddin, A., Tsuji, N., 2023. Peatland groundwater level in the Indonesian maritime continent as an alert for El Niño and moderate positive Indian Ocean dipole events. Sci. Rep. 13 (1), 939. https://doi.org/10.1038/s41598-023-27393-x.
Sulistyanto, Y. (2004). Nutrient dynamics in different sub-types of peat swamp forest in Central Kalimantan, Indonesia (Ph.D. Thesis). University of Nottingham, Nottingham, United Kingdom.
Sumarga, E., Hein, L., Hooijer, A., Vernimmen, R., 2016. Hydrological and economic effects of oil palm cultivation in Indonesian peatlands. Ecol. Soc. 21 (2), 52. https://doi.org/10.5751/ES-08490-210252.
Sunaryathy, P.I., Suhasman, S., Kanniah, K.D., Tan, K.P., 2015. Estimating aboveground biomass of oil palm trees by using the destructive method. World J. Agric. Res. 3 (1), 17–19. https://doi.org/10.12691/wjar-3-1-4.
Supari, Tangang, F., Salimun, E., Aldrian, E., Sopaheluwakan, A., Juneng, L., 2018. ENSO modulation of seasonal rainfall and extremes in Indonesia. Clim. Dyn. 51 (7), 2559–2580. https://doi.org/10.1007/s00382-017-4028-8.
Sutton, O.F., Petrone, R.M., Devito, K.J., 2024. Mining and climate change alters water storage and streamflow dynamics of northern peatland-dominated catchments. Water Resour. Res. 60 (12), e2024WR037266. https://doi.org/10.1029/2024WR037266.
Swails, E., Hertanti, D., Hergoualc'h, K., Verchot, L., Lawrence, D., 2018. The response of soil respiration to climatic drivers in undrained forest and drained oil palm plantations in an Indonesian peatland. Biogeochemistry 142, 37–51. https://doi.org/10.1007/s10533-018-0519-x.
Sweet, W.V., Park, J., 2014. From the extreme to the mean: acceleration and tipping points of coastal inundation from sea level rise. Earth's. Future 2 (12), 579–600. https://doi.org/10.1002/2014EF000272.
Tahir, Z., Haseeb, M., Mahmood, S.A., Batool, S., Abdullah-Al-Wadud, M., Ullah, S., Tariq, A., 2025. Predicting land use and land cover changes for sustainable land management using CA-Markov modelling and GIS techniques. Sci. Rep. 15 (1), 3271.
Tang, A.C.I., Stoy, P.C., Hirata, R., Musin, K.K., Aeries, E.B., Wenceslaus, J., Shimizu, M., Melling, L., 2019. The exchange of water and energy between a tropical peat forest and the atmosphere: seasonal trends and comparison against other tropical rainforests. Sci. Total Environ. 683, 166–174. https://doi.org/10.1016/j.scitotenv.2019.05.217.
Taufik, M., Veldhuizen, A.A., Wösten, H.H.M., van Lanen, H.A.J., 2019. Exploration of the importance of physical properties of Indonesian peatlands to assess critical groundwater table depths, associated drought and fire hazard. Geoderma 347, 160–169. https://doi.org/10.1016/j.geoderma.2019.04.001.
Thompson, J.R., Sorenson, H.R., Gavin, H., Refsgaard, A., 2004. Application of the coupled MIKE SHE/MIKE 11 modelling system to a lowland wet grassland in southeast England. J. Hydrol. 293, 151–179. https://doi.org/10.1016/j.jhydrol.2004.01.017.
Treby, S., Jayasekara, C., Idrus, N.I., Ningsih, S.N.A., Graham, L.L.B., Hutley, L.B., Beringer, J., Grover, S., 2025. Hydrological Fluxes From a Drained Tropical Peatland: Evapotranspiration Consistent Despite Large Fluctuations in Precipitation and Soil Moisture. Hydrol. Process. 39 (10), e70240. https://doi.org/10.1002/hyp.70240.
Vogt, P., Riitters, K., Estreguil, C., Kozak, J., 2024. Revisiting the landscape mosaic model. PLOS ONE 19 (5), e0304215. https://doi.org/10.1371/journal.pone.0304215.
Wahyono, S.C., Kurnain, A., Nata, I.F., Asyari, M., 2023. Post peat fire soil natural recovery based on physical properties in South Kalimantan, Indonesia. Int. J. Plant Soil Sci. 35 (18), 1416–1424. https://doi.org/10.9734/IJPSS/2023/v35i183409.
Wijedasa, L.S., Sloan, S., Page, S.E., Clements, G.R., Lupascu, M., Evans, T.A., 2018. Carbon emissions from Southeast Asia peatlands will increase despite emission reduction schemes. Glob. Change Biol. 24 (10), 4598–4613. https://doi.org/10.1111/gcb.14340.
Wooster, M.J., Gaveau, D.L.A., Salim, M.A., Zhang, T., Xu, W., Green, D.C., Huijnen, V., Murdiyarso, D., Gunawan, D., Borchard, N., Schirrmann, M., Main, B., Sepriando, A., 2018. New tropical peatland gas and particulate emissions factors indicate 2015 Indonesian fires released far more particulate matter (but less methane) than current inventories imply. Remote Sens. 10 (4), 495. https://doi.org/10.3390/rs10040495.
Wösten, J.H.M., Hooijer, A., Siderius, S., Rais, D.S., Idris, A., Rieley, J., 2006. Tropical peatland water management modelling of the Air Hitam Laut catchment in Indonesia. Int. J. River Basin Manag. 4 (4), 233–244. https://doi.org/10.1080/15715124.2006.9635293.
Wösten, J.H.M., Ritzema, H.P., 2001. Land and water management options for peatland development in Sarawak, Malaysia. International Peat. Journal 11, 59–66.
Xiao, H.M., Lo, M.H., Yu, J.Y., 2022. The increased frequency of combined El Niño and positive IOD events since 1965s and its impacts on maritime continent hydroclimates. Sci. Rep. 12 (1), 7532. https://doi.org/10.1038/s41598-022-11663-1.
Xu, L., Sun, S., Chen, H., Chai, R., Wang, J., Zhou, Y., Ma, Q., Chotamonsak, C., Wangpakapattanawong, P., 2021. Changes in the reference evapotranspiration and contributions of climate factors over the Indo–China Peninsula during 1961–2017. Int. J. Climatol. 41 (15), 6511–6529. https://doi.org/10.1002/joc.7209.
Yan, J.J., Smith, K.R., 1994. Simulation of integrated surface water and ground water systems – model formulation. Water Resources Bulletin, 30 (5), 879–890. https://doi.org/10.1111/j.1752-1688.1994.tb03336.x.
Yupi, H.M., Inoue, T., Bathgate, J., 2016. Concentrations, loads and yields of organic carbon from two tropical peat swamp forest streams in Riau Province, Sumatra, Indonesia. Mires Peat 18, 14. https://doi.org/10.19189/MaP.2015.OMB.181.
Zhang, L., Dawes, W.R., Walker, G.R., 2001. Response of mean annual evapotranspiration to vegetation changes at catchment scale. Water Resour. Res. 37 (3), 701–708. https://doi.org/10.1029/2000WR900325.
Zimmermann, B., Zimmermann, A., Scheckenbach, H.L., Schmid, T., Hall, J.S., Van Breugel, M., 2013. Changes in rainfall interception along a secondary forest succession gradient in lowland Panama. Hydrol. Earth Syst. Sci. 17 (11), 4659–4670. https://doi.org/10.5194/hess-17-4659-2013.